ELSEVIER

Journal of South American Earth Sciences 25 (2008) 1–21

Journal of
South American
Earth Sciences

www.elsevier.com/locate/jsames

Morphodynamics of the Pacific and Caribbean deltas of Colombia, South America

Juan D. Restrepo [a,*], Sergio A. López [b]

[a] *Department of Geological Sciences, EAFIT University, Medellín AA 3300, Colombia*
[b] *Master Program in Earth Sciences, EAFIT University, Medellín, Colombia AA 3300, Colombia*

Received 16 January 2007; accepted 24 September 2007

Abstract

This paper analyzes the physical factors controlling the recent morphology of major deltas along the Pacific and Caribbean coasts of Colombia. The study considers the fluvial, coastal, and oceanographic contributions to changes in delta morphology and uses different approaches, including (1) remote sensing techniques; (2) time series analysis of river discharge, sea level, wave climate and tidal variability; (3) analysis of the relationship between monthly mean sea level anomalies near the deltas related to the El Niño Southern Oscillation (ENSO); (4) development of a database of key physical variables; (5) series of correlation calculations to examine which environmental factors control delta morphology; (6) analysis of shoreline changes for the 1986–2000 yr-period; and (7) classification of each delta system based on the relationship between water and sediment discharges and wave and tidal energies. Overall, Colombian deltas are built under destructive physical conditions. The Pacific deltas, San Juan, Mira, and Patía, are tide-influenced deltas although they exhibit definite characteristics of wave-dominated systems such as the presence of barriers and beach ridges. Also, these deltas exhibit the highest marine energy conditions of all Colombian deltas (marine power values between 9.1 and 11.6) due to the interplay of (1) moderate wave conditions as a result of the effect of swells from the SW with a significant height varying from 1.7 in the San Juan delta to 3.0 m and 3.1 m in the Mira and Patía deltas, respectively; (2) meso-tidal ranges; (3) steep subaqueous profiles; (4) low attenuation indexes of deep-water waves; and (5) strong oceanographic manifestations associated with the ENSO, causing regional sea level rises of 20–44 cm during El Niño events. The Caribbean deltas, Magdalena, Sinú and to a lesser extent, the Atrato, are wave-influenced deltas. The Magdalena, with deep and nearshore wave power values of 45×10^6 erg s^{-1} and 35×10^6 erg s^{-1}, respectively, and the lowest attenuation index of deep-water waves, is the most wave-influenced delta of Colombia. Statistical relationships show that the area of Colombian deltas is best predicted from average discharge and bank-full width of river entering the delta. The number of distributary channels is explained by the marine power index and the gradient of the delta plain. The average and total width of distributary channels are largely controlled by the tidal range. Further analysis of shoreline changes indicate that the retreating behavior of the western part of the Magdalena delta has been due to anthropogenic causes, including the construction of jetties in 1936. By contrast, processes of rapid erosion in the San Juan delta have been the result of 2.6 mm yr^{-1} long-term relative sea level rise due to tectonic induced subsidence coupled with a eustatic rise of sea level. Overall, the other deltas are experiencing prograding phases with rates of accretion of 100 m yr^{-1} in the artificial delta of the Canal del Dique.

Keywords: Colombia; Deltas; Pacific coast; Caribbean coast; Delta morphodynamics; Discharge; Waves; Tides; Relative sea level; El Niño; Recent delta evolution

1. Introduction

The morphology of deltaic systems is controlled by the interaction of local factors (Wright and Coleman, 1973; Wright, 1977; Galloway, 1975; Syvitski et al., 2005a,b): (1) water and sediment discharge rates reflecting drainage characteristics such as climate, morphology, and tectonism; (2) receiving basin characteristics, including bathymetry, slope of continental margin, isostasy, subsidence, sea-level changes, and tectonics; (3) coastal processes such as wave

* Corresponding author. Tel.: +57 4 2619329; fax: +57 4 2664284.
E-mail address: jdrestre@eafit.edu.co (J.D. Restrepo).

0895-9811/$ - see front matter © 2007 Elsevier Ltd. All rights reserved.
doi:10.1016/j.jsames.2007.09.002

and tidal energy, and longshore and cross-shelf currents; and (4) density differences between river and coastal waters relevant in controlling the dynamics of fluvial plumes.

Many models have been used to classify the morphology of deltas by analyzing the dynamics of fluvial discharges and their transport mechanisms. The ternary diagram proposed by Galloway (1975), illustrates the division of deltas into fluvial-dominated, wave-dominated, and tide-dominated. Orton and Reading (1993) modified Galloway's approach and used a new classification system based on sediment grain size of delta deposits. Other classification schemes have included new variables such as changes in sea level (Postma, 1995), or quantitative indexes of mean tidal range and mean wave height (Hori and Saito, 2008).

According to Syvitski (2005), a problem associated with many schemes of delta classification has been the difficulty to obtain a global view of deltas. The morphology of several deltaic systems has been described in a qualitative manner based on environmental factors and geomorphological patterns. Many deltas are not well known and lack quantitative databases of key morphodynamic factors associated with their recent evolution. These deltas are mainly located in developing countries, and basic research on these systems has been slow to start (Hori and Saito, 2008). Colombia is not the exception. There are no scientific descriptions of physical processes in river deltas along the Pacific and Caribbean coasts of Colombia. The San Juan is the only delta that has been partially documented in terms of morphodynamics (Restrepo and Kjerfve, 2000a, 2002; Restrepo et al., 2002).

The morphology and recent evolution of the Colombian deltas (Fig. 1) are unique when compared to other deltas of South America because of the singular combination of extreme climatic, geological, and oceanographic conditions in which the deltas are built, including (1) high tectonic activity with the occurrence of shallow earthquakes and tsunamis (Kellogg and Mohriak, 2001); (2) narrow continental shelves with limited accommodation space (Correa, 1996); (3) drainage basins with high rates of precipitation, water discharge and sediment load (Restrepo and Kjerfve, 2000a); (4) the complexity of littoral dynamics resulting from micro and mesotidal ranges (Kjerfve, 1981; Restrepo and Kjerfve, 2002; Restrepo et al., 2002), and the effect of significant swells and associated coastal currents (Restrepo et al., 2002); (5) strong oceanographic manifestations associated with the ENSO cycle, causing sea level rises during

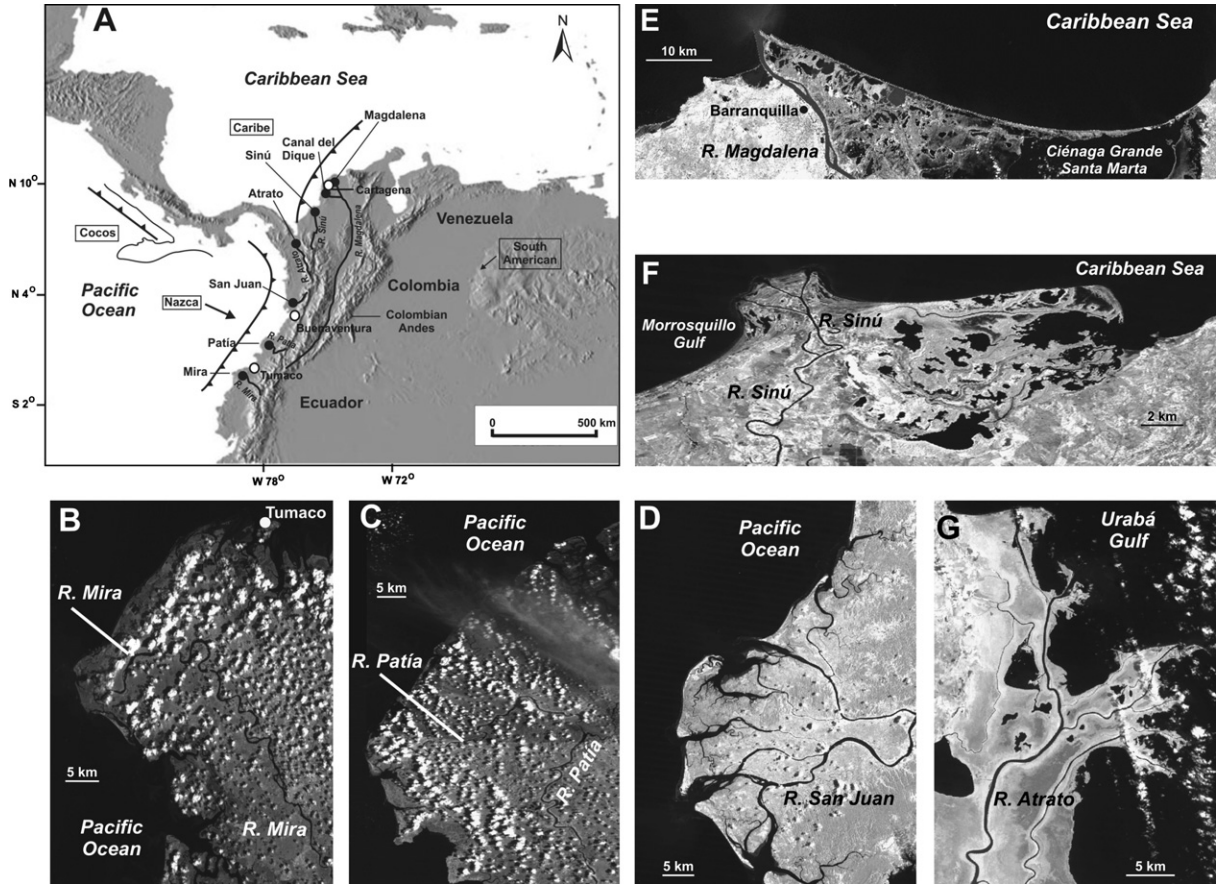

Fig. 1. (A) Map of the Pacific and Caribbean coasts of Colombia, showing the locations of the principal river deltas (solid circles), the tectonic setting of the coasts, and the tidal gauges at Tumaco, Buenaventura, and Cartagena (white circles). (B–G) Satellite images of the six river deltas analyzed in this study, including Mira (B), Patía (C), San Juan (D), Magdalena (E), Sinú (F), and Atrato (G). All imagery is from Landsat satellite supported by the University of Maryland.

El Niño years (Morton et al., 2000); and (6) increasing rates of relative sea level (Restrepo et al., 2002). It is worth noting that although the occurrence of high energetic and destructive conditions along the Colombian coasts, small to medium-sized rivers (e.g., Magdalena River) form extensive deltas (Fig. 1).

This study focuses on the morphodynamics of major deltas in Colombia, the Mira, Patía, and San Juan deltas on the Pacific coast, and the Atrato, Sinú, and Magdalena on the Caribbean coast (Fig. 1). Our primary goal is to identify the principal factors determining the recent morphology of these deltas. We also present a database of key physical factors, classify each delta based on quantitative indices, discuss the morphology and recent delta evolution, and compare Colombian deltas with major global systems.

2. Major deltas and their physical setting

The major Pacific deltas from north to south are the San Juan, Patía, and Mira (Fig. 1). Their drainage basins are located within the humid tropics, characterized by high but relatively constant temperature, high rainfall rates, and high humidity. Average rainfall in the entire Pacific basin ranges from 2000 to 12,700 mm yr^{-1} (Snow, 1976; Restrepo and Kjerfve, 2000a). The entire Colombian Pacific coast is characterized by high tectonic activity and prograde on a narrow shelf bordering a deep trench. Along the northern margin, the Nazca oceanic plate is converging with the South American continental plate at a rate of 54 mm yr^{-1} (Kellogg and Mohriak, 2001) (Fig. 1A). The convergence has produced an unstable coast characterized by the occurrence of large magnitude, shallow focus earthquakes. Severe earthquakes, accompanied by destructive tsunamis, impacted the Colombian coast in 1836, 1868, 1906, 1979, and 1991 (Pennington, 1981; Lockridge and Smith, 1984; Kellogg and Vega, 1995; Meyer et al., 1992; INGEOMINAS, 2005).

The Pacific rivers have lobate littoral barred deltas (Fig. 1). The San Juan delta with an emergent area of ~800 km^2 and a shoreline of 51 km (Fig. 1D), is classified as an intermediate system (Galloway, 1975) and also as a type III (Coleman, 1981). The delta is influenced differentially by fluvial discharge, wave energy and tides at its several distributary mouths (Restrepo et al., 2002). The Patía (Fig. 1C), a deltaic system influenced by tectonic activity and with a sub-aerial area of ~820 km^2, has been classified as a tide-dominated delta. The Mira (~443 km^2) is an intermediate system but with a higher contribution of wave forces (Vernette et al., 2002) (Fig. 1B). These deltas consist of distributary channels flanked by tropical humid forests, mangrove swamps, tidal flats, and barrier islands.

Caribbean Colombia is principally drained by the Magdalena, Sinú, and Atrato rivers (Fig. 1). The Magdalena River measures 1612 km and drains a 257,438 km^2 basin, which occupies a major portion of the Colombian Andes. It is the largest fluvial system in Colombia and originates from headwaters in the Andean Cordillera at an elevation of 3,300 m. The Atrato, draining a basin of 35,700 km^2, occupies a considerable portion of the Pacific basin, but the river empties into the Caribbean via the Urabá Gulf. The Sinú River empties into the Morrosquillo Gulf and drains an area of 10,180 km^2.

The Caribbean drainage basins are characterized by high and moderate rainfall patterns averaging 4944, 1750, and 2050 mm in the Atrato, Sinú, and Magdalena watersheds, respectively (Table 1). The climate of the region is modulated by the geographical position of the Intertropical Convergence Zone (ITCZ). The seasonality of the position of the ITCZ corresponds to the windy and dry (December–April) and rainy (August–October) seasons. The rest of the year is transitional between these two seasons. In the dry season the ITCZ resides at its southernmost position (0–5°S). At that time the northern trade winds dominate the area with average speeds of ~8 m s^{-1} and diurnal peaks up to ~15 m s^{-1} (Andrade, 1993). During the rainy season the ITCZ moves over the southwestern Caribbean, decreasing the wind speed of the southerlies there and promoting the highest rate of precipitation anywhere in the western hemisphere (Andrade and Barton, 2000).

The Caribbean region is also characterized by the convergence of the South American and the Caribbean

Table 1
River length (L), drainage basin area (A), basin maximum elevation (R), average annual precipitation (r), water discharge (Q), monthly maximum water discharge (Q_{max}), runoff (Δf), runoff coefficient ($\Delta f/r$), suspended sediment load (Q_s, and basin wide sediment yield (Y) for the major deltas along the Pacific and Caribbean coasts of Colombia

Fluvial system/Delta	L (km)	A (km^2)	R (m)	r (mm yr^{-1})	Δf (mm yr^{-1})	$\Delta f/r$ (–)	Q (m^3 s^{-1})	Q_{max} (m^3 s^{-1})	Q_s ($\times 10^6$ t yr^{-1})	Y (t km^{-2} yr^{-1})
Pacific coast										
Mira	272	9530	3346	4703	2872	0.61	868	3270	9.7	1025
Patía	415	23,700	4580	3296	1718	0.52	1291	3082	21.1	972
San Juan	352	16,470	3900	7277	4884	0.67	2550	5000	16.4	1150
Caribbean coast										
Atrato	700	35,700	3150	4944	2420	0.49	2740	3060	11.3	315
Sinú	300	14,700	3350	1750	800	0.46	373	586	4.2	589
Magdalena	1540	257,440	3300	2050	886	0.43	7232	10287	144	560

The location of each delta is shown in Fig. 1

tectonic plates (Fig. 1). The Caribbean margins of Panama, Colombia, and Venezuela consist of extensive fold belts (Case et al., 1971). The North Panama and North Colombia fold belts are characterized by numerous volcanoes that are formed by overpressured Miocene muds and occasionally capped with reefs. Also, seismic sections across the Panama deformed belt reveal that Panama is continuing to collide eastward with the northern Andes. The Panama–Colombia border area near the Atrato delta is one of the most seismically active areas in northwestern South America (Kellogg and Mohriak, 2001).

The Magdalena, an arcuate delta with an emergent area of 1690 km^2, is the largest delta in Colombia (Fig. 1E). This delta is classified as wave-dominated system (Coleman, 1981) and consists of alluvial plains, marginal lagoon systems and beach ridges (Vernette, 1985). The receiving basin is characterized by sedimentation, slumping and compressional tectonics that cause the presence of mud diapirism in the delta front (Shepard et al., 1968; Kolla and Buffler, 1984; Vernette et al., 1992). The delta mouth empties into an offshore canyon with a steep slope (40°) (Shepard, 1973). The Sinú delta with a sub-aerial area of ~26 km^2 is classified as a river and wave-dominated system (Coleman, 1981; Vernette et al., 2002) (Fig. 1F). In contrast with the Magdalena River, which delivers all its sediments over the continental slope, the Sinú delivers its sediments into the largest portion of the continental shelf (Tabares et al., 1996; Serrano, 2004). The Atrato River delta (Fig. 1G), with an area ~672 km^2 and located west of the Sinú (Fig. 1), is a river-dominated delta with a bird-foot morphology (Vernette et al., 2002).

3. Methods

Our approach considers the fluvial, coastal, and oceanographic contributions to changes in delta morphology. To assess morphometric characteristics, shoreline changes and how delta geomorphology has changed during the last two decades, satellite images of each of the 6 deltas were processed from Landsat 7 imagery (30 m pixel resolution or mpr) obtained from the Global Land Cover Facility of the University of Maryland. Also, aerial photographs (1–3 m pixel resolution), maps at scale 1:25,000, and SPOT imagery (10 mpr) were examined. More than three temporal images from the space of each deltaic system were analyzed to identify geomorphic characteristics of the distributary channels connected to the main fluvial river. The images were rectified to 1:50,000 topographic maps (Geographic Institute of Colombia, IGAC) after establishing ground control points. The geo-registered images were corrected for atmospheric path radiance by subtracting band minimum values from within the darkest topographic shadows. The ERDAS Image 8.1 software was used for image analysis and to estimate rates of coastal retreat and progadation. In addition, shoreline changes along the San Juan delta were documented using radar images from 1968 and 1992, air photographs from 1968, 1993, and 1997, and interviews with inhabitants.

The climatic pattern of each delta system was examined by obtaining daily temperature and rainfall data (1970–2001) from the Hydrological Institute of Colombia (IDEAM) for many stations throughout the drainage basins. In addition, monthly water discharge and sediment load data were obtained from the IDEAM for the most downstream station at each river (IDEAM, 1995), or from various studies (Restrepo and Kjerfve, 2000a,b; Restrepo et al., 2002; Restrepo, 2005).

To compare and contrast the physical processes occurring in the delta distributaries, we made observations along the main distributary channels and their inlets of the Pacific deltas, including San Juan and Mira. Because of logistic constraints, we did not take measurements along the Patía river delta. The measurements consisted of time series measurements of currents, temperature, salinity, and water level elevation at two stations in the San Juan delta and four stations in the Mira delta using an InterOcean S4 electromagnetic current meter with CTD (including high-precision depth capability) and a Nortek acoustic wave and current meter AWAC (including a pressure sensor with resolution of 0.25%). The instruments were deployed at the center of each navigational channel and maintained 1 m above the bottom. Also, hourly sea level data were obtained from tidal gauges at Buenaventura (1955–2000), Tumaco (1954–2000), and Cartagena (1955–2000) (Fig. 1) (University of Hawaii Sea Level Center/NOAA). The data were approximately 92% complete, and missing data were interpolated with harmonic analysis (Franco, 1988, 1992).

To assess tidal variability in other deltaic systems such as the Atrato, Sinú, and Magdalena, we obtained tidal predictions done by IDEAM in stations located at each delta front. We subjected the water level data to harmonic analysis to calculate amplitude and phase of tidal constituents, and the main tidal statistics (Franco, 1988, 1992; Pugh, 2004). In addition, meteorological and far-field low frequency responses were obtained by using an eighth-order recursive Butterworth low-pass filter with 38-h half-power gain to suppress semidiurnal and diurnal tidal variability (Schwing et al., 1983). To assess the relative astronomical water level variability, we summed the variance of the semidiurnal, diurnal, shallow water harmonic constituents, $\sum A_i^2/2$, to obtain the astronomical tidal variance, and then divided by the total variance in the time series.

With respect to wave data along the Caribbean and Pacific coasts of Colombia, we are not aware of any published measurements of waves. To remedy this, we obtained wave data around each delta for the 1963–2000 period from the NOAA-Comprehensive Ocean-Atmosphere Data Set (COADS, releases 1 and 1a) (Woodruff et al., 1987, 1993, 1998). The data were obtained from the World Meteorological Observation, Voluntary Observing Ships Program. The data include 56,980 sets of observations of wind speed and direction, swell and wave direction, period, and height.

To address the morphodynamic characteristics of the Colombian deltas, we developed a database of key physical variables according to the environmental factors established by Syvitski (2005) and Syvitski et al. (2005a,b): (1) drainage area of each delta system (A); (2) maximum relief of the watershed (R); (3) basin climate temperature (T); (4) basinwide precipitation (r); (5) runoff (Δf); (6) runoff coefficient ($\Delta f/r$); (7) average water discharge (Q); (8) monthly maximum water discharge (Q_{max}); (9) average suspended sediment load (Q_s); (10) basinwide sediment yield (Y); (11) length of the main course of the river (L); (12) gradient of the delta plain (D_{grd}); (13) number of distributary channels (C_N); (14) width of the distributary channels (C_W); (15) bank-full width of river entering the delta (R_W); (16) spring ($K_1 + M_2$) tidal range (T_i); and (17) maximum monthly wave height (W_a). Other physical variables, including trend in relative sea level (S_L) and sea level anomalies (S_{LA}) related to El Niño-Southern Oscillation (ENSO), were calculated to evaluate the impact of changing sea level on delta morphology.

To obtain predictive relationships and examine which environmental factors control delta morphodynamics, series of correlation calculations were done using the database from the six deltas (Tables 1 and 4). Both single and multiple correlations were performed. Pearson correlation coefficients were calculated for some variable pairings for delta properties and for the neperian logarithm of delta variables. To analyze if a significant component of some delta variables can be explained by a combination of several controls, a step-wise regression was implemented on the database. Here we examine a set of estimator variables, select those that are most efficient at explaining the variance in a response variable, and build them into a model.

The morphodynamic classification of Colombian deltas was done by using two approaches, including (1) the shoreline classification system (e.g., Davies and Hayes, 1984; Hori et al., 2002) and (2) the quantitative relationships between log mean tidal range/mean wave height versus log suspended sediment load, and log water discharge (Hori and Saito, 2008). The latter approach assumes that all deltas should be strongly influenced by fluvial discharge and sediment load. Thus, the well-known delta type "fluvial dominated" used in the Galloway's ternary diagram (Galloway, 1975) is not adopted in this scheme. Instead, it classifies deltas into three types: wave influenced; mixed wave and tide influenced; and tide influenced.

The trend in relative sea level along the Pacific and Caribbean coasts was estimated by least-squares linear regression for the Buenaventura, Tumaco, and Cartagena time series. To evaluate the monthly mean sea level anomalies near the deltas related to ENSO, we removed mean monthly values to eliminate seasonal effects. A filtered sea level was calculated by subtracting the interannual mean sea level for each month (S^*) from the respective monthly mean sea level in each year (S) for the ith month of the jth year to form the deviation from the long-term monthly mean sea level $S'_{ij} = S_{ij} - S^*_i$ (Quinn et al., 1978; Enfield and Allen, 1980). The Southern Oscillation Index (SOI) data were obtained from the National Oceanic and Atmospheric Administration-NOAA (2005) (http://ffp.ncep.noaaa.gov/pub/cpc/wd52dg/data/indices).

In order to compare Colombian deltas with South American and major global deltaic systems, we used the database of physical factors that control delta morphology for the major global deltas (Syvitski, 2005). Thus, we calculated the river ($Q_{max}D_{grd}$) and marine ($W_a^2 + T_i^2$) power indexes, and the ratio of sediment supply to marine dispersal (Q_s:P_m) (Syvitski, 2005).

4. Results and discussion

4.1. Water discharge and sediment supply

The extreme climatic conditions along the Pacific basins of Colombia are responsible for the high water discharge into the Pacific. The largest is the San Juan with a mean discharge of 2550 $m^3\ s^{-1}$. The Patía has a mean river basin discharge of 1291 $m^3\ s^{-1}$, and Mira River contributes an average 839 $m^3\ s^{-1}$. Table 1 shows the drainage areas, main climatic characteristics, and water discharge and sediment load for the largest Pacific and Caribbean rivers.

Sediment flux to the coastal zone is conditioned by geomorphic and tectonic influences (basin area and relief), geography (temperature, runoff), geology (lithology, ice cover), and human activities (reservoir trapping, soil erosion) (e.g., Milliman and Syvitski, 1992; Syvitski et al., 2005a,b; Syvitski and Milliman, 2007). On a global basis, the warm temperate region has the highest sediment yield of all the climate zones and accounts for nearly 2/3 of the global sediment delivery. Also, river basins draining high mountains (>3000 m) contribute ~60% of the global sediment flux to the coastal zone (Syvitski et al., 2005a,b).

The Pacific deltas are built by small rivers with high sediment yield (Table 1). The San Juan occupies a 16,465 km^2 basin with the highest mean sediment load (16×10^6 t yr^{-1}) and basin-wide sediment yield (1150 t $km^{-2}\ yr^{-1}$) on the entire west coast of South America (Restrepo and Kjerfve, 2000a). The Patía River, with a drainage area of 23,700 km^2, has a sediment load and basin-wide sediment yield of 14×10^6 t yr^{-1} and 972 t $km^{-2}\ yr^{-1}$, respectively. Based on daily measurements from 1982 to 2000 by IDEAM at Pipiguay, which only covers 4% of the upstream basin, the upper portion of Mira River has an annual sediment load of 213,160 t yr^{-1} and a sediment yield of 507 t $km^{-2}\ yr^{-1}$. This sediment yield is much lower than the yield of 856 t $km^{-2}\ yr^{-1}$ estimated by Restrepo and Kjerfve (2000a,b), which only included 10 years of data 1982–1992. According to John Milliman (pers. commun.) both estimates do not reflect the denudation rates present in these humid drainage basins of western Colombia. In addition, these yields do not express the conditions of deposition and storage that occur in the entire basin. To remedy this, we estimated sediment load for the Mira River catchment from the regression of sediment load on basin

area for tropical rivers with precipitation rates higher than 700 mm yr^{-1} (Latrubesse et al., 2005). The best estimate for the total sediment load into the Pacific Ocean from the Mira is 9.7 MT yr^{-1}. This results in a sediment yield estimate of 1025 t km^{-2} yr^{-1}, very similar to the yields of 1150 t km^{-2} yr^{-1} and 980 t km^{-2} yr^{-1} estimated by Restrepo and Kjerfve (2000a,b) for the San Juan and Patía rivers, respectively.

Along the Caribbean, the sediment load of the Atrato River is 11.3×10^6 t yr^{-1}, and the corresponding sediment yield 315 t km^{-2} yr^{-1} (Table 1). The sediment yield is comparatively low, because of the large size of the drainage basin and the extensive low-lying Urabá alluvial flood plains, with an area of 5500 km^2, where significant sediment deposition and storage occur. The annual discharge and sediment load of the Sinú River are 373 m^3 s^{-1} and 6×10^6 t yr^{-1}, respectively, with a basin-wide sediment yield of 589 t km^{-2} yr^{-1} (Table 1). Daily water discharge measurements in the Magdalena River, 1942–2000, indicate an annual discharge of 7232-m^3 s^{-1}. Load measurements during the 1972–1998 year-period yielded an annual sediment load of 144×10^6 t yr^{-1}. The calculated sediment yield for the entire drainage basin area is 560 t km^{-2} yr^{-1} (Table 1).

In general, climate determines where tropical weathering occurs, while tectonics increase erosion rates and dictate the composition of erosion products (Stallard, 1988). Drainage basins with intense tectonic activity usually have high sediment yields (Meade, 1988; Milliman and Syvitski, 1992), as in the case of Colombian rivers. Furthermore, the presence of unstable and cation-rich minerals in the suspended load and bedload of rivers draining the Andean basins suggests that rapid erosion is indeed occurring. Thus, along the slopes of the Pacific and Caribbean basins, high temperatures, humid conditions, and abundant vegetation in these high rainfall basins promote rapid chemical weathering and high denudation rates.

Besides climate and weathering factors, other processes such as landslides lead to slumps that increase sediment loads. In humid uplands, landslides are the dominant mass wasting process (Hovius et al., 1997; Hovius et al., 1998). The Colombian Pacific basins are characterized by the presence of active fault systems, high precipitation rates (reaching as much as 12 m in the Atrato watershed), slopes frequently steeper than 35°, and dense tropical rain forests (West, 1957; Correa, 1996). According to Hovius et al. (1997), these conditions are favorable to the occurrence of rapid mass wasting caused mainly by hillslope erosion processes such as landslides, slumps and slides.

The trend between delta area and drainage basin area for the Colombian river deltas were determined by log–log regression of delta area on basin area. Fig. 2a indicates that Colombian deltas fit the global trend well. The small Pacific rivers, including the Atrato, show a clear cluster. Although the Atrato discharges into the Caribbean Sea, its drainage basin is located west of the Cordilleras and has the same drainage basin characteristics as the San Juan

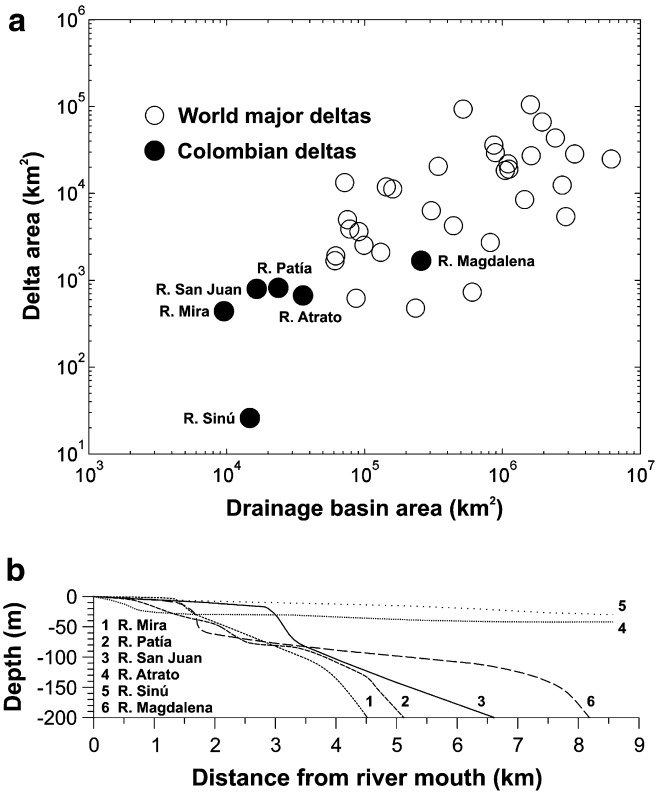

Fig. 2. (a) Relationship of drainage basin area (km^2) and delta area (km^2) for the major Colombian and global river deltas. Data for the world's major deltas were obtained from Syvitski (2005). (b) Bathymetric profiles of subaqueous deltas based on bathymetric maps from the hydrographic service of the Colombian Navy (unpublished data).

and Patía rivers (e.g., headwaters at high elevations, high rainfall rates, and high tectonic activity). Even though these rivers drain small basins they have high sediment yield and construct extensive deltas. Over a distance less than 75 km, the San Juan River falls abruptly from an elevation of 3900 m to 100 m. Likewise, the Patía descends from its headwaters at 4580 m elevation to 400 m over a distance of 150 km. Thus, the control exerted by narrow alluvial plains results in less sediment deposition/storage within the drainage basins.

With respect to sediment budgets in deltas and sediment supply to the oceans, 10–30% of sediment load of large rivers passing the farthest downstream gauging stations are trapped in delta plains of subaerial deltas and river channels. Subaqueous deltas may trap 70–80% of sediment load passing the farthest downstream gauging stations (Hori and Saito, 2008). Based on the late Holocene depositional history of the San Juan delta, which was inferred from the analysis of 11 hammer cores (González and Correa, 2001), and assuming an average thickness of 7 m for the entire 800 km^2 of the sub aerial delta and a constant sediment supply for ~5000 year period, Restrepo et al. (2002) showed that the sediment load delivered to the San Juan delta would have been $\sim 5.7 \times 10^{10}$ m^3. According to their assumptions, this implies that only 10% of the river sediment was captured in the subaerial delta and that 90%

was trapped in the subaqueous delta. In the Sinú delta, however, Serrano (2004) obtained an estimated net sediment accumulation of 161×10^6 m^3 and an estimated sedimentation rate of 2.83×10^6 m^3 yr^{-1} for the 1957–1997 year-period. According to this study, most accumulation occurred in the subaerial delta (~70%). For the other Colombian deltas there are no rough estimates of sediment budgets and accumulation patterns in the subaerial and subaqueous margins.

4.2. Marine forcing factors

4.2.1. Tidal characteristics

The results of the water level harmonic analyses are presented in Table 2. The analysis of tidal characteristics from two gauging stations in the Pacific deltas indicates that these deltas have meso-tidal range, ranging from 3.0 to 1.3 m. The tidal phase for the major diurnal and semidiurnal constituents progresses from north to south along the coast, with high water first occurring in San Juan and later in the Mira delta, consistent with a southward propagating Kelvin wave along western South America (Pugh, 2004). Water level inequality (Schurman, 1941) occurs prominently in high waters only in San Juan. The tides in these two deltas are pure semidiurnal with a form number (ratio of the main diurnal and semidiurnal component amplitudes, $K_1 + O_1/M_2 + S_2$; Defant, 1960) varying from 0.18 to 0.09.

The hourly time series at the San Juan delta indicate a pronounced 15–16 day periodicity. However, low-frequency water level fluctuations are less significant at the Mira delta. In the mouth of the San Juan, processes at tidal frequencies explain 75% of total water level variability, with semidiurnal, diurnal and shallow water constituents explaining 60%, 2%, and 13%, respectively. Seasonal, meteorological and river discharge variability account for 25% of the water level variance. In the mouth of the Mira River, the semidiurnal and diurnal constituents represent 88% of the water level variance, and 12% is due to meteorological factors. Further analysis indicates that in the San Juan inlet, tidal asymmetry is caused by distortion of the tide by runoff and bathymetry, resulting in an appreciable M_4 shallow water tidal component with amplitude of 55 cm. At the Mira delta, however, the M_4 tidal component is only 0.3 cm and water level asymmetry is negligible, reflecting differences in the morphology of the two delta mouths (Table 2).

The analysis of tidal characteristics from 4 locations in the Caribbean deltas indicates that these systems have micro-tidal range, ranging from 62 to 15 cm. The tide is primarily diurnal in the Atrato and Sinú deltas with a form number of 5.5 and 4.9, respectively. In the Magdalena delta

Table 2
Main water level tidal harmonic constants in the major deltas of Colombia, where H_n (cm) is amplitude and g_n is the phase lag (°G) of the equilibrium tide at Greenwich (Pugh, 1987)

Constituent	Origin	Period (solar hours)	Pacific coast		Caribbean coast		
			Mira H_n (cm)/g_n (°)	San Juan H_n (cm)/g_n (°)	Atrato H_n (cm)/g_n (°)	Sinú H_n (cm)/g_n (°)	Magdalena H_n (cm)/g_n (°)
Diurnal							
Q_1	Larger elliptical lunar	26.87	0.7/293	6/161	1/72	6/254	13/269
O_1	Principal lunar	25.82	0.5/256	6/240	33/299	33/300	23/258
K_1	Principal solar–lunar	23.93	0.6/101	25/039	33/301	36/289	35/270
Semidiurnal							
N_2	Larger elliptical lunar	12.66	4/185	25/169	10/251	5/222	9/126
M_2	Principal lunar	12.42	6/98	137/323	7/259	8/302	28/21
S_2	Principal solar	12.00	116/198	31/208	5/230	6/86	4/211
L_2	Smaller elliptical lunar	12.19	20/53	6/266	15/55	1/61	9/76
K_2	Declinational lunar–solar	11.97	32/177	8/199	1/228	2/97	1/198
Shallow water							
MK_3			0.7/22	7/196	133/198	115/14	140/172
MN_4			0.6/44	16/338	104/89	59/94	70/63
M_4	Principal lunar over-tide	6.21	0.3/359	55/117	157/110	163/92	178/100
MS_4		6.10	1.5/13	26/360	23/342	43/340	17/255
M_6			0.2/98	13/073	28/236	35/254	57/245
$2MS_6$			0.2/56	9/313	21/333	17/346	32/78
M_8			0.2/96	8/068	43/339	48/300	65/41
$3MS_8$			0.1/61	11/325	43/11	33/292	27/14
Tidal statistics	*Formula*						
Form number (–)	$(K_1 + O_1)/(M_2 + S_2)$		0.09	0.18	5.5	4.93	1.81
Inequality phase (°)	$M_2^\circ - (K_1^\circ + O_1^\circ)$		−259	43	−341	−287	−507
Phase age (°)	$0.98 * (S_2^\circ - M_2^\circ)$		98	−112	28.4	−211.68	186.2
Mean tidal range (m)	$2.2*(M_2)$		1.3	3.0	0.15	0.18	0.62
Spring tidal range (m)	$2.0*(M_2 + S_2)$		2.4	3.4	0.24	0.28	0.64
Neap tidal range (m)	$2.0*(M_2 - S_2)$		1.1	2.1	0.04	0.04	0.48

the tide is a mixed primarily diurnal tide with a form number of 1.9 (Table 2). In general, the diurnal component tides are largely uniform in both phase and amplitude for most of the Caribbean deltas.

4.2.2. Wave climate

Wave data indicate that the observed waves in the Pacific deltas are predominantly swells from the southwest (63–68%) with a significant height varying from 1.7 in the San Juan delta to 3.0 m and 3.1 m in the Mira and Patía deltas, respectively. Average swell height is 1.4 ± 0.7 m, and the mean period ranges from 6.1 ± 2.6 s in the San Juan delta to 6.3 ± 2.6 s in the Mira delta. The maximum heights are considerably higher for swells with values ranging up to 7.5 m. In the Caribbean, the deltas are mostly impacted by swells from the northeast (36–78%). Average swell height varies from 2.3 ± 1.2 m in the Magdalena delta to 1.6 ± 0.8 in the Atrato. Significant and maximum heights are considerably higher in the Magdalena delta with values of 5.1 m and 9.0 m, respectively (Table 3).

The general configuration of a delta shoreline cannot be explained by the characteristic of a single set of waves (height, period, and direction). In order to relate morphology to wave energy, it is necessary to express the wave regime in terms of long-term statistical averages of wave power (Wright and Coleman, 1971). The wave power climate can be expressed by combining the effects of all datasets of wave characteristics for each month. This is done by taking the monthly weighted means of the total and longshore power values. The methods to estimate wave-power are shown in Wright and Coleman (1971, 1974).

The analysis of total wave power per unit crest width along each delta front indicates that the Magdalena delta has the higher nearshore wave power with 35×10^6 erg s^{-1} m. Also, wave power at the 9 m depth contour is higher in the Magdalena (45×10^6 erg s^{-1} m) than any value observed along the other deltas considered in this study. In addition, the Pacific deltas exhibit moderate wave energy conditions with an average wave power of $\sim 16 \times 10^6$ erg s^{-1} m at the 9 m depth contour (Table 3).

The depositional form of deltas depends on the magnitude and distribution of wave forces, as well as the rate of sediment supply. If sediment load is small and wave energy high, the waves will mold the river-borne sediment into a marine-dominated coastline. If, on the other hand, river sediment discharge is high compared to wave forces, the river will build a protruding delta (Wright and Coleman, 1973; Coleman, 1981). In general, the greater the river discharge, the greater the wave power required to rework the sediment into a wave-dominated configuration (Wright and Coleman, 1972). Although the Pacific deltas have a high rate of sediment discharge, swells with a significant height between 1.7 m and 3.0 m create a marine-dominated coast with beach ridges, spits, and barrier islands.

In addition, if sediment load peaks coincide with times of greatest wave power, the increased supply of sediment may be balanced more closely by the capacity of the waves to redistribute sediments. If river discharge and maximum wave power are out of phase, then the river outflow may dominate for part of the year, and this condition will be followed by a period of intense reworking by waves. The former situation should favor a more regular and smooth progradation of the delta shoreline, whereas the latter situation would be more likely to lead to the formation of successive spits, barrier islands, or beach ridges along the coast flanking the river mouths (Wright and Coleman, 1974).

Fig. 3 shows the river discharge/wave-power climate analysis for the Colombian deltas. In the Pacific systems, the disparity between wave power and discharge power probably has a fundamental effect on the development of periodic coastline features such as beach ridge systems adjacent to the distributary mouths. In contrast, the Atrato and Sinú deltas are characterized by periods of maximum discharge approximately in phase with times of maximum wave power. The dominance of river discharge is therefore moderate most of the year. However, some distinct peaks of fluvial discharge are out of phase with nearshore wave power between June and August. The events of this short period are probably responsible for the pronounced seaward protrusion of these two deltas. In the Magdalena delta, the shoreline is extensively reworked by wave processes. The dimensionless discharge and wave power curves are only slightly out of phase. The maximum river discharge peaks in November while wave power has its maximum value in December (Fig. 3f). Furthermore, wave dominance is evident in the landscapes of the Magdalena with a deltaic plain consisting of beach ridges and dunes composed of clean and well-sorted sands. The delta has succeeded in building a slight protrusion in the vicinity of the river mouth and its coastline has been straightened and made regular by wave activity (Fig. 1E).

Observations along the subaqueous deltas of major rivers, including the Amazon (Nittrouer et al., 1996), the Mahakam (Storms et al., 2005), the Ganges–Brahmaputra (Kuehl et al., 1997), the Po (Cattaneo et al., 2003), and the Fly (Harris et al., 2004), suggest that the depositional mechanisms of subaqueous deltas are controlled by energetic marine environments, which are related to energetic waves and meso–macro tidal ranges. Each subaqueous delta is different in size and morphology due to differences in fluvial discharge, shelf bathymetry, and the local oceanographic regime (Storms et al., 2005). Fig. 2b shows that the shape of the Colombian deltas may be entirely flat (Atrato and Sinú river deltas), smoothly curved (Mira and Patía river deltas) or angular-shaped (San Juan and Magdalena river deltas). Probably, the deeper depths of the delta-front platform of the Magdalena, San Juan and Mira deltas may be attributed to the high and moderate wave energy on the delta coast (Table 3).

Wave power may be attenuated substantially over the broad, gently sloping sub-aqueous profiles which are facing most large river deltas (Coleman, 1981). By flattening the offshore slope through the addition of sediment, the river can oppose the marine forces more effectively. Where rivers

Table 3
Values and rms variability of wave height and period at seas and swells near the major deltas of Colombia

Wave characteristics	Pacific coast			Caribbean coast		
	Mira	Patía	San Juan	Atrato	Sinú	Magdalena
Seas	Sea/swell wave	Direction				
Predominant Sea direction (1963–2000)	SW (195°–254°)	SW (195–254°)	SW (220.5–265.5°)	NW (285°–344°)	NE (015–074°)	NE (015–074°)
Mean height (m) ± rms	0.9 ± 0.5	0.9 ± 0.5	0.9 ± 0.4	0.8 ± 0.4	1.4 ± 0.8	1.6 ± 0.9
Maximum height(m)	3.0	2.5	2.7	1.5	6.5	6.5
Significant height (m)	2.0	2.1	1.4	1.8	3.3	3.6
Mean period (s) ± rms	5.2 ± 1.4	5.5 ± 1.5	5.6 ± 1.2	5.0	6.0 ± 1.8	6.1 ± 1.8
Swells						
Predominant Swell direction (1963–2000)	SW (195°–254°)	SW (195–254°)	SW (220.5–265.5°)	NE (015–074°)	NE (015–074°)	NE (015°–074°)
Mean height (m) ± rms	1.4 ± 0.6	1.4 ± 0.7	1.4 ± 0.7	1.6 ± 0.8	2.1 ± 1.3	2.3 ± 1.2
Maximum height (m)	4.5	6.5	7.5	6.5	9.0	9.0
Significant height (m)	3.0	3.1	1.7	3.6	4.9	5.1
Mean period (s) ± rms	6.3 ± 2.6	6.3 ± 2.4	6.1 ± 2.6	6.3 ± 2.5	6.5 ± 2.3	6.7 ± 2.3
Wavelength (m)	61.9	61.9	58.0	61.9	48.9	70.0
% Swell direction (1963–2000)	64.2	67.8	63.2	36.0	74.5	77.9
Other wave parameters (shallow water)						
Δx, Incremental linear distance (m, from $d = L/2$ to $d = 9$ m)	529	1167	1250	4375	1818	
Wave height after frictional attenuation (m, Δx to $d = 9$ m)	1.3	1.3	1.3	1.4	1.8	2.1[a]
W_P, Wave power (10^6 erg s^{-1}, $d = 9$ m)	16.2	16.0	15.8	18.5	34.4	45.4[a]
Δx, Incremental linear distance (m, from $d = L/2$ to $d = 0.3$ m)	1765	2833	3250	5417	5727	
Wave height after frictional attenuation (m, Δx to $d = 0.3$ m)	0.25	0.26	0.21	0.14	0.11	4.0[a]
W_P, Wave power (10^6 erg s^{-1}, $d = 0.3$ m)	0.13	0.14	0.10	0.04	0.02	34.9[a]
A_P, Attenuation index (–)	2056	1894	2454	7676	25 376	24[a]

Note: Data for the 1963–2000 yr-period were obtained from the NOAA-COADS/ICOADS, based on 56,980 sets of data points (Woodruff et al., 1987, 1993, 1998). d = depth in shallow water (m); L = wave length (m). Wave height after frictional attenuation over an incremental distance (Δx), wave power (W_P) and attenuation index (A_P) were calculated from predominant swells, based on Wiegel (1948), Wright and Coleman (1971, 1973) and USACE (2002).

Predominant compass direction, wavelength in deep water, wave power and attenuation index are also shown.

[a] For the Magdalena delta, wave power and attenuation index were calculated using the linear theory of waves, which takes into account the swell height after refraction and shoaling (USACE, 2002).

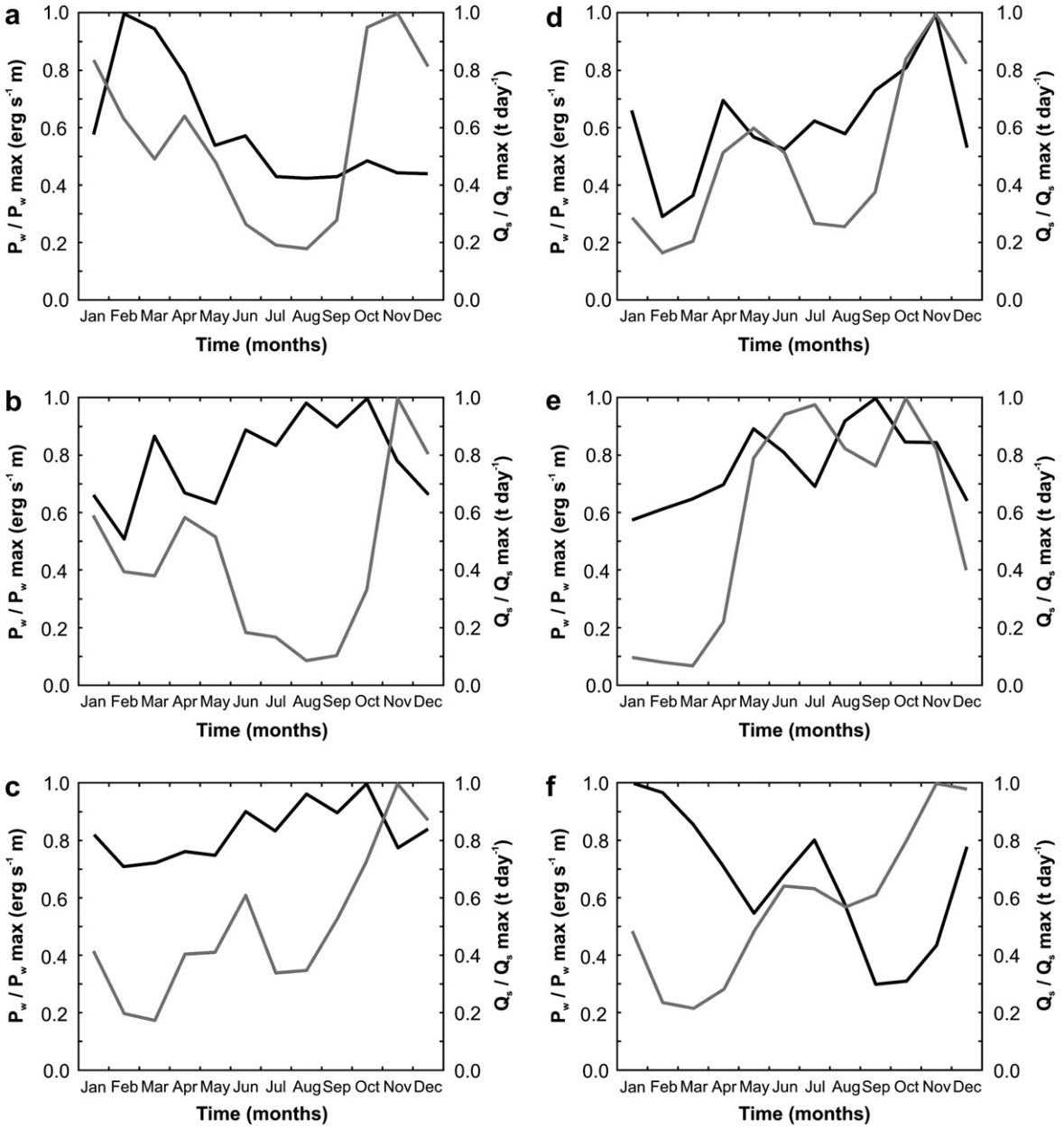

Fig. 3. Sediment load (gray line)/nearshore wave power (bold line) analysis of the river deltas of Colombia, including Mira (a), Patía (b), San Juan (c), Atrato (d), Sinú (e), and Magdalena (f).

discharge large volumes of sediment into broad and shallow continental shelves, friction reduces incident waves to a lesser extent before they reach the shore (Wright and Coleman, 1973). The subaqueous profiles of Colombian deltas show close relationship with subaerial delta morphology. Slopes are gentle and convex seaward of the river-dominated delta systems, such as those of the Atrato and Sinú (Fig. 2b). As offshore profiles become steeper and more concave, wave-dominated coastline features, including beach ridges and spits, become more prominent. In the Pacific and Magdalena River deltas, coastal irregularities and protrusions decrease as a result of increasing offshore slope and consequently increasing nearshore wave power (Fig. 2b, Table 3).

The degree to which wave power is reduced by the offshore slope is indexed by an attenuation ratio (A_P). This index, developed by Bretschneider (1954) and Bretschneider and Reid (1954), estimates the reduction of wave height due to bottom friction (Wright and Coleman, 1973). In the Pacific deltas the attenuation ratios indicate that friction reduces nearshore power to 19% and 25% of the deep-water power, while in the Atrato and Sinú deltas, the A_P values are higher and wave power is reduced by 77% and 90%, respectively (Table 3). In contrast, the steeper profile in the Magdalena River delta causes low reduction of wave power due to friction. This morphologic condition may be responsible for the lowest attenuation ratio of any Colombian delta (Fig. 2b, Table 3).

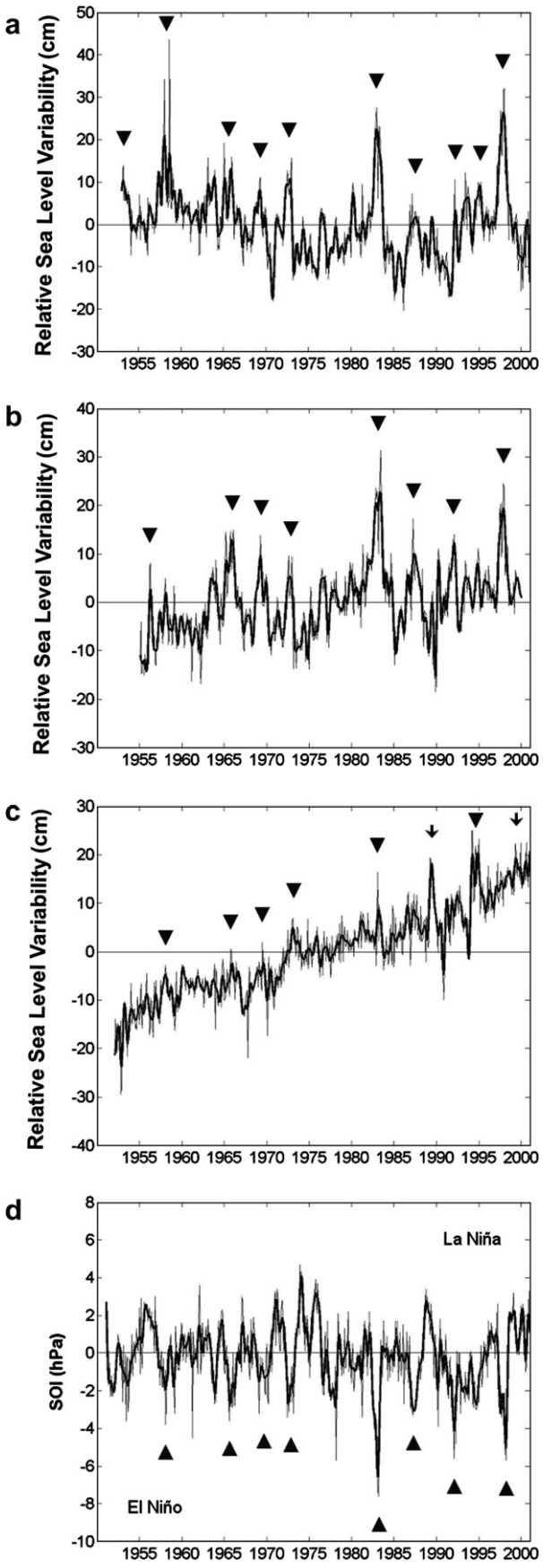

4.2.3. Sea level anomalies related to ENSO

The impact of ENSO on the eastern Pacific sea level has been documented for 1950–1974 (Enfield and Allen, 1980), 1955–1973 (Wyrtki, 1975), 1970–1975 (Wyrtki, 1977), and 1982–1983 (Cane, 1983). Observations have shown that El Niño 1997–1998 raised sea level by 20–30 cm along the Pacific coast of Colombia (Martínez et al., 2000; Morton et al., 2000). The intensities of ENSO events are classified on the basis of high sea-surface temperatures (SST) and atmospheric pressure differences between Tahiti and Darwin (SOI). Anomalously low values of the SOI correspond to periods of weakened trade winds and positive anomalies of temperature and sea level in the eastern Pacific (Quinn et al., 1978; Enfield and Allen, 1980; Glantz, 1997). At Tumaco and Buenaventura (Fig. 1), high sea level anomalies and the SOI index show good coherence for the 46-year period 1954–2000 (Fig. 4). Regression analysis between the smoothed sea level and the smoothed SOI yielded a coefficient of variation of $R^2 = 0.61$ in Tumaco and $R^2 = 0.54$ in Buenaventura, both coefficients significant at the 95% confidence level, which indicates that variations in the SOI explain 61% and 54% of the seasonal variability in water level, with low values of SOI corresponding to high Tumaco and Buenaventura sea level anomalies (Fig. 4a and b). Thus, the sea levels in the Mira and San Juan deltas are strongly affected by the Southern Oscillation.

The 1982 El Niño in the eastern equatorial Pacific was remarkable. By October SST was almost 5 °C above normal and the sea level at the Galapagos Islands had risen by 22 cm (Cane, 1983). Also, during the 1998 El Niño, equatorial waters in the eastern Pacific were 3–4 °C warmer and 20–30 cm higher than normal (Morton et al., 2000). In Tumaco (Fig. 4a), strong El Niños in 1982 and 1998 raised sea levels by 28 cm and 32 cm, respectively, while in Buenaventura (Fig. 4b), these El Niño events raised sea levels by 33 cm and 27 cm. Moderate El Niño events in 1958, 1965, 1969, 1972, 1987, and 1992 raised the water level by 10–44 cm along the Mira and San Juan river deltas (Fig. 4). According to Restrepo et al. (2002), positive sea level anomalies in the San Juan delta during 1998 increased the frequency of washover and flooding to at least twice per month. Channel migration and beach retreat intensified dramatically and the agricultural land and the majority of houses were lost to beach erosion. Although sea level anomalies in Cartagena show a weak correlation with the SOI index ($R^2 = 0.28$), the El Niño events in 1982 and 1995 raised sea levels by 15 cm and 25 cm, respectively.

Fig. 4. Time series plots of water-level anomalies at Tumaco (a), Buenaventura (b), and Cartagena (c) in 1954–2000. (d) The Southern Oscillation Index (SOI), the atmospheric pressure difference (milibar) at sea level between Darwin, Australia, and Tahiti. The SOI data were obtained from the National Oceanic and Atmospheric Administration-NOAA (2005) (http://ffp.ncep.noaaa.gov/pub/cpc/wd52dg/data/indices).

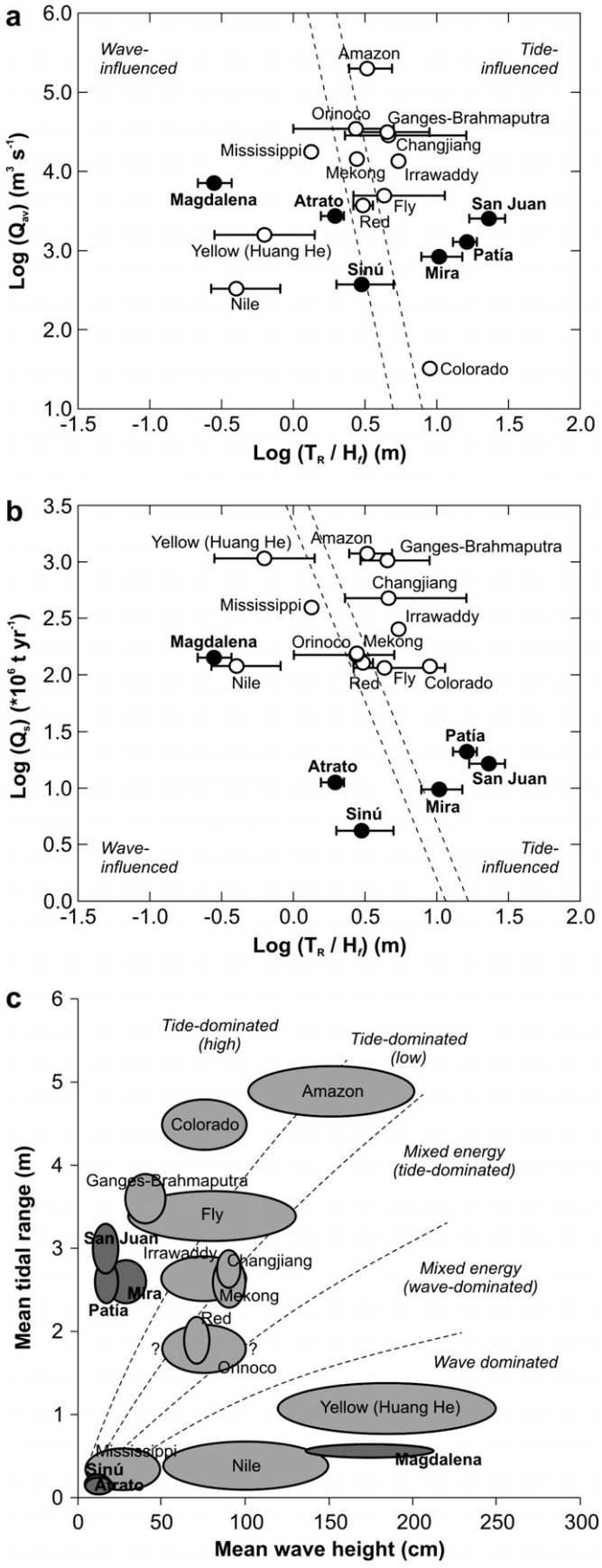

4.3. Delta classification

Fig. 5 shows the morphologic classification of Colombian deltas done by using the quantitative relationships between log mean tidal range/mean wave height versus log suspended sediment load, and log water discharge (Hori and Saito, 2008). Wave-influenced Colombian deltas are the Magdalena and Sinú. Although the Atrato exhibits bird's-foot topography, it shows the contribution of wave forces due to the low tidal energy present along its shoreline (Table 2). Marshes, swamps, and lakes are the most abundant features in this delta and wave-deposited sand features such as beaches and beach ridges are scarce. Toward the wave-dominated end of the spectrum there is a progressive decrease in river-dominated features such as digital distributaries, bays, and marshes and an increase of wave-built features such as beach ridges, spits, dunes, and barrier islands. The Sinú delta, like the Atrato, is characterized by marshes and lakes, but the coastline is smoother and sand features such spits and beach ridges are much more developed than in the Atrato. However, fluvial dominance is still evident and reflected by the pronounced cuspate form of the Sinú delta and by the mangroves which dominate around the flanks of bays and behind the sand beaches of the delta shoreline. The Magdalena River has built an elongated and arcuate delta at its mouth and wave dominance is evident in the landscapes of the delta plain. The Magdalena has succeeded in building only a slight protrusion in the vicinity of the river mouth where sand barriers, beaches, and dunes are the most common features of the deltaic plain. Thus, the Magdalena delta exhibits definite characteristics of wave dominance (Fig. 5).

Tide-influenced deltas are common along the Pacific coast and exhibit funnel-shaped river mouth morphology. Although the San Juan, Patía, and Mira deltas have significant river-produced bulges, their shorelines have been smoothed into regular and rounded forms by wave activity. Continuous beach and beach-ridge formations fringe the coastline of these deltas. An interesting feature arising from this classification scheme is the contribution of wave energy to the morphology of Pacific deltas. Even though these systems are not classified as mixed wave-and- tide influenced deltas, their coasts have been intensely eroded and reworked by wave action. Also, most of the Colombian deltas, except Mira and Sinú, show large contributions of fluvial discharge due to its location up in the classification diagram (Fig. 5).

Fig. 5. Classification diagrams for major Colombian deltas plotting mean tidal range/mean wave height versus log water discharge (a) and log suspended sediment load (b). The dashed lines divide the three types of deltas, including wave-influenced (left side), mixed tide and wave-influenced (center), and tide-influenced deltas (right side) (after Hori and Saito, 2008). (c) Mean wave height versus mean tidal range for major Colombian deltas. The regions are grouped into five morphological categories (after Davies and Hayes, 1984; Hori et al., 2002).

4.4. Environmental variables controlling delta morphology

Based on our physical database (Tables 1 and 4), the best predictors of delta area (A_D) across the Colombian deltas are water discharge Q ($m^3\ s^{-1}$) and bank-full width of river entering the delta R_W (m) and explain 97% of the data variance (Eq (1): Table 5). The first-order control of water discharge on delta areas was also shown by Syvitski (2005). In this study of 55 global deltas, variables explaining most variation in observed delta areas were average water discharge (78%) and the total sediment load (3%). Since we did not calculate the total sediment load (suspended sediment load and bedload), these two estimators, Q and R_W reflect the transport capacity of the fluvial system.

It has been argued that a relevant factor controlling the three-dimensionality of deltas is the number and pattern of distributary channels (e.g., Gould, 1979; Kanes, 1970, cited by Syvitski et al., 2005a,b). In addition, the number of distributary channels found on a delta plain is limited by wave energy and the dispersal mechanisms of the river bedload (e.g., longshore transport). Therefore, an inverse relationship is to be expected between wave action and channel number (Bhattacharya and Giosan, 2003; Syvitski et al., 2005a,b). For the Colombian deltas, the number of distributary channels is inversely predicted by the marine power (P_W) accounting for 45% of the data variance (Eq. (3): Table 5). It is positively affected by the gradient of the delta plain D_{grd} (39%). Thus, if the marine power is small, then over time more distributary channels will be built. In addition, the width of distributary channels, C_W, is largely explained by tidal range, T_i, and to a lesser extent by water discharge and C_N ($R^2 = 0.99$; Eq. (4): Table 5). Tidal range was also the most important estimator predicting the total width of distributary channels, TC_W ($R^2 = 0.88$; Eq. (5): Table 5). On a global basis, T_i was also the main variable explaining channel width. Tidal currents and water discharge are relevant controls keeping the channel mouths enlarged (Syvitski, 2005). Finally, the gradient of the delta plain, D_{grd}, was positively correlated with bank-full width of river entering the delta (R_W, 29%) and nearshore wave power (W_P, 28%), and inversely affected by water discharge (34%) ($R^2 = 0.91$; Eq. (2): Table 5).

4.5. Shore dynamics and human impacts

During the 3–4 last decades, the barrier islands of the San Juan delta have experienced important morphological changes similar to changes in all the barrier islands along the Pacific coast of Colombia (Martínez et al., 1995, 2000). Shoreline changes along the delta front reflect both erosional and accretionary events, documented in air photographs from 1968, 1993 and 1997, and interviews with inhabitants. Major changes have occurred to the south in the Chavica and San Juan distributaries (Fig. 6a). From 1968 to 1997, the position and morphology of the delta front changed significantly as reflected by (1) the formation

Table 4
Database of morphodynamic factors associated with major deltas in Colombia, including delta area (A_D), gradient of the delta plain (D_{grd}), delta width (D_W), number (C_N) and width (C_W) of distributary channels, bank-full width of river entering the delta (R_W), shelf width (S_W), length of the coastline (L_C), spring tidal range (T_i), maximum monthly wave height (W_a)

Delta	A_D (km^2)	D_{grd} ($\times 10^{-5}$ m m^{-1})	C_N (–)	D_W (km)	C_W (m)	R_W (m)	S_W (km)	L_C (km)	T_i (m)	W_a (m)	P_r	P_m	Q_s:P_m	P_m:P_r	S_L (mm yr^{-1})	S_{LA} (cm)
Pacific coast																
Mira	443	4.85	5	34	617	400	11.4	50	3.0	0.36	0.35	9.13	0.0008	26.09	−1.14	28–32
Patía	820	15.48	6	57	1500	600	10.0	62	3.0	0.24	0.25	9.06	0.074	36.24		
San Juan	800	13.79	5	40	2240	400	6.7	51	3.4	0.23	0.69	11.60	0.045	16.81	2.26	27–33
Caribbean coast																
Atrato	672	4.87	7	42	117	500		112	0.24	0.17	0.15	0.09	5.10	0.60		
Sinú	26	20.40	3	11	267	120		17	0.28	0.12	0.12	0.09	1.48	0.75		
Magdalena	1690	7.66	3	67	510	600	2.0	77	0.64	2.70	0.79	7.86	8.02	9.95	5.98	15–25

The indexes of marine power (P_m) and river power (P_r), the ratio of sediment supply to marine dispersal (Q_s:P_m) (Syvitski, 2005), and the trends in relative sea-level (S_L) and the highest sea-level anomalies related to the El Niño-Southern Oscillation (S_{LA}) are also shown. We only show values of S_L and S_{LA} for those deltas near the tidal gauges at Buenaventura, Tumaco, and Cartagena (Fig. 1).

Table 5
Models and estimator variables predicting delta area (A_D), gradient of the delta plain (D_{GRD}), number (C_N), width (C_W), and total width (TC_W) of distributary channels in the Pacific and Caribbean river deltas of Colombia

Model	R^2	F-Value	p-Value
$A_D = -4.973E^{-11} + 0.696\,\overset{87\%}{Q}\,0.397\,\overset{10\%}{R_W}$	0.97	46.27	0.0056
$D_{grd} = 3.722E^{-10} - 2.551\,\overset{34\%}{Q} + 0.682\,\overset{29\%}{R_W} + 1.700\,\overset{28\%}{W_a}$	0.91	6.36	0.1388
$C_N = 4.101E^{-10} - 0.859\,\overset{45\%}{P_W} + 0.639\,\overset{39\%}{D_{grd}}$	0.84	7.65	0.0664
$C_W = -1.642E^{-11} + 1.210\,\overset{64\%}{T_i} - 0.470\,\overset{24\%}{D_{grd}} - 0.372\,\overset{11\%}{C_N}$	0.99	54.08	0.0182
$TC_W = -1.144E^{-18} + 0.938\,\overset{88\%}{T_i}$	0.88	29.37	0.0056

Note: Q, water discharge; R_W, bank-full width of river entering the delta; P_W, marine-power index; W_a, maximum monthly wave height; T_i, spring tidal range.

of an extensive sandy cuspate tidal flat extending seaward 1.2 km at the Chavica mouth; (2) a 1.5 km spit actively growing toward the southeast from the San Juan mouth; (3) a 150–220 m retreat of the beach along the 2 km central segment of El Choncho barrier island; and (4) opening of a new inlet during a spring washover event.

In the past few decades, the central segment of the El Choncho part of the delta has retreated at 4 m yr^{-1} for as much as 100 m (Neal and González, 1990). Erosion from April 1993 to November 1997 has been documented by topographic profiles. Beach retreat has narrowed the barrier island by 60 m (an average rate of 11 m yr^{-1} for the period), destroying citrus and coconut plantations, and houses that were built more than 0.5 m above the highest spring tides (Restrepo et al., 2002). On the other hand, the opening of a new inlet occurred in June 1996, during an exceptionally high tide. The island was incised by a small channel, 5 m wide and 0.5 m deep. The channel grew rapidly with each high tide, and by December 1996, it had become a true inlet, 30 m wide and several meters in depth. By May 1997, the inlet had migrated to the south and had reached a width of 50 m and a depth of 10 m (Correa and González, 2000; Restrepo et al., 2002). A strong bi-directional tidal circulation deposited an ebb tidal delta in front of the inlet, and the sand drift to the south became even more disrupted. By December 1997, flooding along the central part of El Choncho destroyed several houses, and by February 1998, the central part of the island was permanently inundated with the inlet continuing to migrate to the south. In addition, high sea levels and strong currents have destroyed fringing mangroves (Restrepo et al., 2002). Overall, major morphological changes have occurred in the San Juan delta during this 29-year period, including shoreline retreat, narrowing of barrier islands, and the occurrence of breaching events.

Changes in the Mira delta coastline between 1958 and 2000 are shown in Fig. 6b. Maximum shoreline progradation of approximately 2000 m has occurred at the north section of the river mouth, and maximum erosion of approximately 600 m occurred at the apex of the southern spit. In general, the Mira delta shore has protruded seaward at a rate of 48 m yr^{-1} during the 42-year period. Further analysis of present deltaic evolution shows that the main distributaries are migrating to the south and exhibit widening of the inlets and spit growth on the northern end. Also, the Atrato and Sinú deltas on the Caribbean coast show coastline progradation during the 1986–2002 yr-period. Maximum accretion rates of 1300 m are present in the western part of the Sinú delta (Fig. 6c).

The Caribbean region is characterized by countries ranging from small, low islands to continental, mountainous lands with strong differences in rainfall patterns, climate, landform and land use. The coastal zone supports more than 100 million people in more than 25 countries. In the region, sedimentation and erosion are the most significant coastal issues. The response to coastal problems is usually hard engineering (coastal sea defenses) rather than more environmentally sustainable soft engineering solutions (Kjerfve et al., 2002).

Few deltas remain in their pristine form – most are highly engineered to control flooding both from rivers and from the sea (Syvitski et al., 2005a,b). Other anthropogenic effects include changes in the natural rate of delta accretion through increased sediment supply due to deforestation and agriculture (Restrepo and Syvitski, 2006). Also, rates of delta progradation can increase when the locations of distributary channels are artificially controlled (Syvitski et al., 2005a,b; Restrepo, 2007). In the Magdalena delta, the construction of the Barranquilla port has seriously affected the erosion/accretion equilibrium along the delta front. Levees constructed during the early 1900s to facilitate navigation and create an open channel into the Caribbean have confined the fluvial sediment to the river channel, resulting in the delivery of the available sediment load offshore rather than deposition in the delta shoreline (Alvarado, 2005) (Fig. 7b). Furthermore, the present delta mouth empties into an offshore canyon with a steep slope (40°) (Shepard, 1973). This decrease in sediment delivery is a significant factor contributing to land loss on the western part of the Magdalena delta. Further analysis also indicates that strong littoral currents flowing predominantly toward the west, which are the result of open ocean swells generated by NE trade winds (Table 3) create beach accretion and erosion on the eastern and western sides of the navigation channel, respectively (Fig. 7a). The net estimate of beach erosion on the western part of the delta for the 1936–2002 year period is ~1500 m (Alvarado, 2005; Restrepo, 2007) (Fig. 7b and c). Further analysis of satellite images indicates an average coastal retreat of 55 m yr^{-1} in the western part of the delta for the 1989–2000 yr-period (Fig. 7a).

In general, the San Juan and Mira deltas on the Pacific coast are the only Colombian deltas showing few effects of human presence. Due to the construction of a 5 km-long-channel (Canal Naranjo), which was dredged between the Patía River and the much smaller Sanguianga River to

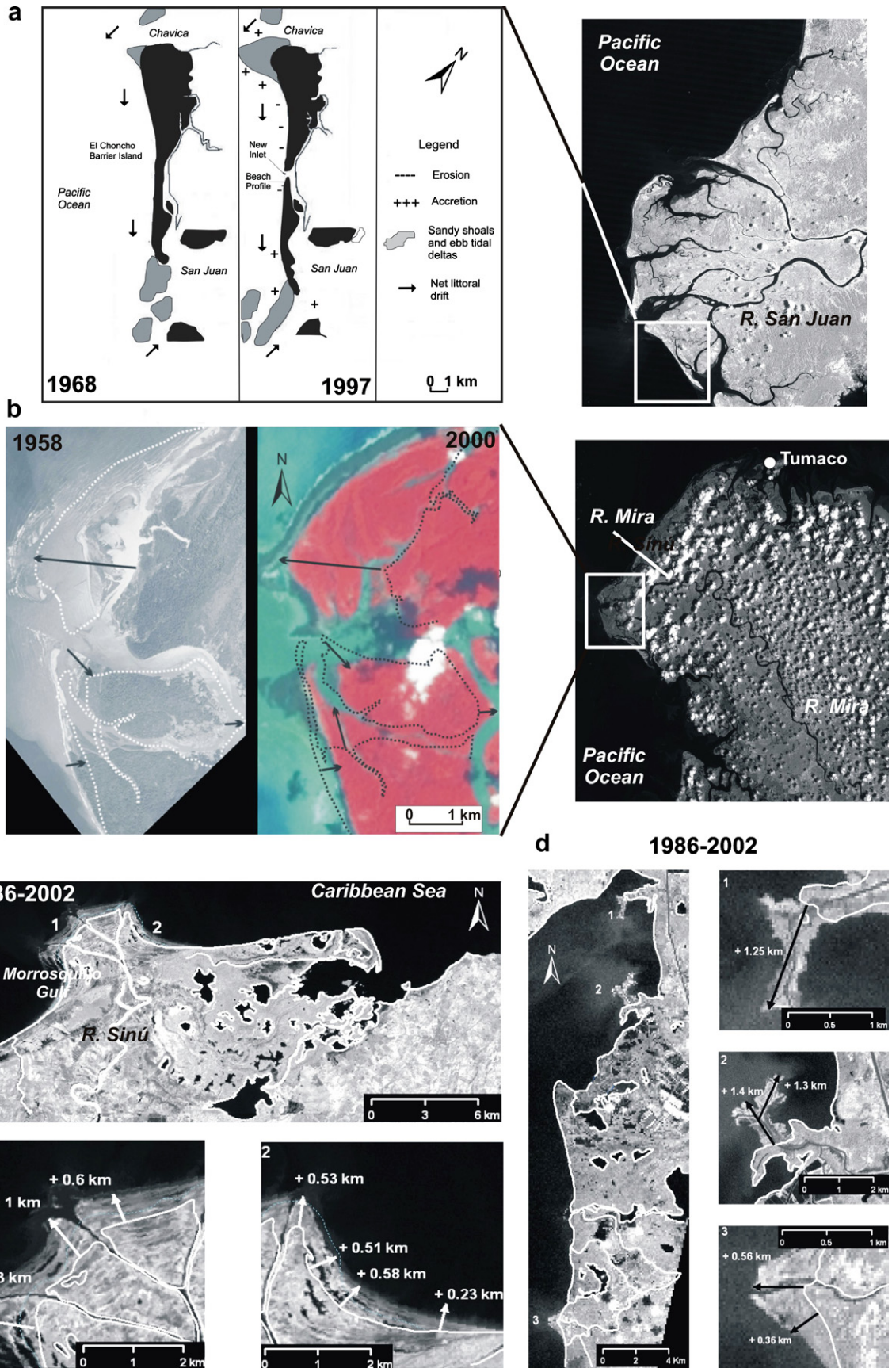

Fig. 6. Major shoreline changes in the San Juan (a), Mira (b), and Sinú deltas (c). Changes in the Canal del Dique delta coastline between 1986 and 2002 are also shown (d). Satellite images of each delta were processed from Landsat 7 imagery (30 m pixel resolution or mpr) obtained from the Global Land Cover Facility of the University of Maryland.

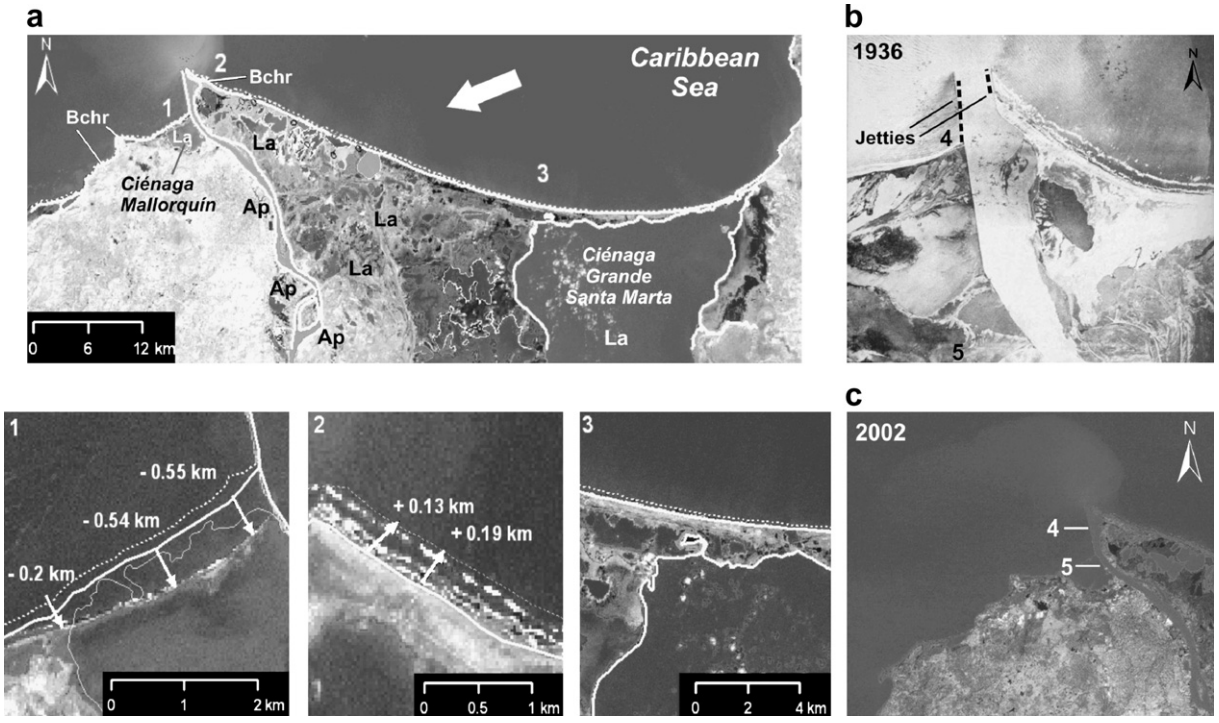

Fig. 7. (a) Satellite image of the Magdalena delta, showing the locations of alluvial plains (Ap), lagoon systems (La) and beach ridges (Bchr), the direction of the NE trade winds (white arrow), and shoreline changes (1–3) between 1989 (dash line) and 2000 (bold line). Satellite images were processed from LANDSAT 5 and 7 data (15–30 m pixel resolution or mpr) and obtained from the Global Land Cover Facility of the University of Maryland; (b) aerial photograph of the Magdalena River mouth from 1936, showing the location of coastal engineering structures and common points (4, 5) also shown in (c); and (c) satellite image of the Magdalena River delta from 2002, showing the location of common points 4 and 5 shown in (b). Note the coastal retreat between 1936 and 2002.

the north in 1976, 117 km upstream of the Patía and 67 km upstream on the Sanguianga, most of the Patía's discharge was captured by the Sanguianga River. This diversion event started during the 1979 earthquake, when the vertical elevations of the basins changed, and the Sanguianga River captured approximately 70% of the Patía's discharge. Since 1979, this diversion has created socioeconomic hardships along the lower courses of both rivers. Impacts included channel erosion, sediment deposition, mangrove die-off, delta-front erosion in the Patía delta, changes in fishing resources, transportation and communication difficulties, and changes in lifestyles (Soeters and Gómez, 1985; Velásquez et al., 1994).

Major anthropogenic impacts on deltas are present on the Caribbean coast. The lower course of the Atrato River and its delta plain has experienced deforestation and soil conversion in the last three decades due to agricultural processes. The largest banana plantations in Colombia are located on the lower Atrato River. Another of the major anthropogenic influences is the artificial delta formed by the Canal del Dique (Fig. 6d). This canal, a 114 km-long man-made channel from the lower course of the Magdalena River to Cartagena Bay (Fig. 1), was constructed in 1650 by indigenous slaves supervised by Spanish conquerors. During the 15 years that it has been monitored (1984–1998), the Canal del Dique has discharged approximately 89×10^6 t of sediment to the Caribbean Sea (Restrepo et al., 2006).

Since the 1930s, the government of Colombia has dredged and reopened the Canal del Dique. Because of increased sedimentation in Cartagena Bay between the 1940s and 1960s, new channels were constructed from El Dique to Barbacoas Bay. These man-made distributary channels formed a river- dominated delta with bird's-foot morphology. In fact, the largest accretion rates of any Colombian delta are observed in the Canal del Dique delta with values up to 1400 m for the 1986–2000 yr-period.

4.6. Trends in relative sea level and its implications

The trend in relative sea level was estimated by least-squares linear regression for the Buenaventura 1955–1999, Tumaco 1953–2000, and Cartagena 1952–2000 time series (Figs. 1 and 8). In Buenaventura the relative sea level rise measured 2.6 mm yr^{-1} and was significant at the 95% level (Fig. 8b), also noted by Aubrey et al. (1988) and Emery and Aubrey (1991). With data extending over shorter time intervals, 1941–1969, Aubrey et al. (1988) determined that the Pacific coast of Colombia near Buenaventura is subsiding by a relative sea level rise of 1 mm yr^{-1}. By contrast, the relative sea level at Tumaco was -1.14 mm yr^{-1}, indicating a decreased trend in sea level for the 47 yr-period (Fig. 8c).

Along the Pacific and Caribbean coasts of Colombia, more than 40 earthquakes with magnitude 4–6 occurred

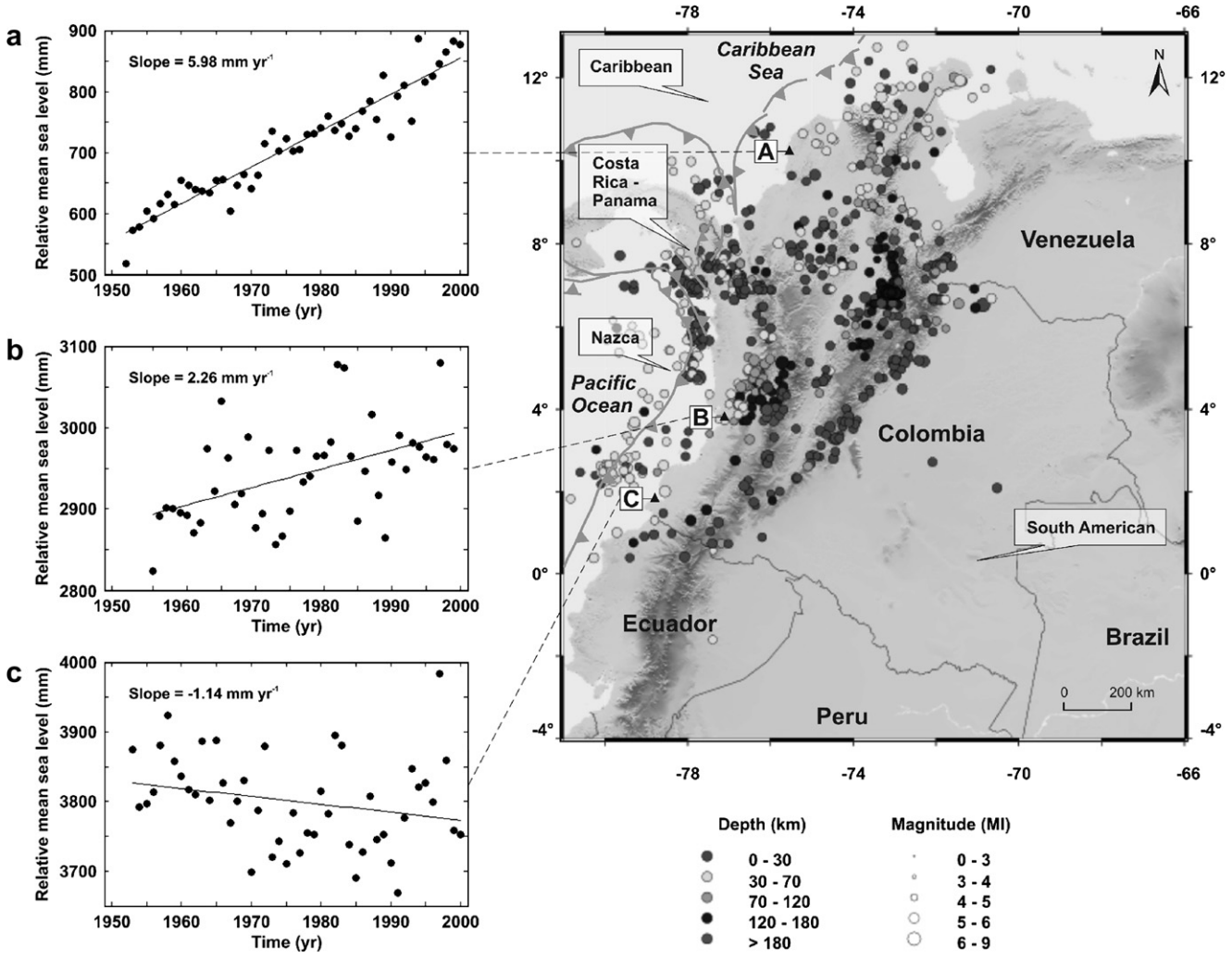

Fig. 8. Mean relative sea-level (mm) from Cartagena (a), Caribbean coast, and Buenaventura (b) and Tumaco (c), Pacific coast of Colombia (University of Hawaii, Sea Level Center Data). (a) Trend line for the 1952–2000 period with slope = 5.98 mm/yr. (b) Trend line for the 1955–2000 period with slope = 2.26 mm/yr. (b) Trend line for the 1953–2000 period with slope = −1.14 mm/yr. We also show the location and magnitude of earthquakes that occurred in Colombia between 1993 and 2003 (d) (Modified from INGEOMINAS, 2005).

within 200 km of the shoreline from 1993 to 2003 (INGEOMINAS, 2005) (Fig. 8d). In the Pacific, the most intensive earthquakes during the 20th century occurred in 1906 and 1979, and caused both regional and local subsidence. Coastal areas of southwestern Colombia, including the shorelines of Tumaco and the Mira delta, subsided as much as 1.6 m, causing an apparent sea level rise along at least a 200 km stretch of the Colombian coast north of the Ecuadorian border (Herd et al., 1992; Correa and González, 2000). The most recent seismic event that impacted this coast occurred in November 1991. It was a magnitude 7.0 earthquake with the epicenter located 40 km north of the San Juan delta at 21 km depth (Meyer et al., 1992). In addition, at least 20 earthquakes with magnitude 4–6 occurred within 100 km of the San Juan delta from 1993 to 2003 (INGEOMINAS, 2005).

It is well documented that when relative sea level increases, deltaic lowlands become more vulnerable to inundation, flood events and erosion (e.g., Day et al., 1995; Ericson et al., 2006). In the Pacific deltas, there are no quantitative measurements of recent coastal subsidence to verify tectonic subsidence (Morton et al., 2000). The principal evidence of subsidence in the San Juan delta (Restrepo et al., 2002), include (1) increased frequency of non-storm overwash on the barrier islands from twice a year (March and October during the highest tides) before the 1991 earthquake to 16 times per year after the 1991 quake; (2) increased erosion of barrier islands with average loss of 11 m yr^{-1} 1993–1997 period; (3) 0.8 m sinking of wooden houses on stilts; (4) post-quake evidence of soil liquefaction, land cracking, and water soil expulsion; (5) an increased trend in relative sea level of 3.4 mm/yr for the 1991–1999 period; and (6) increased mortality of the first line of freshwater trees and mangroves.

Compared to deltas worldwide, the Pacific deltas of Colombia do not experience subsidence due to compaction of underlying sediments, because the deltas are sand-rich systems that lack organics and thick pro-delta mud depos-

its, requisite conditions for substantial subsidence related to compactation (Morton et al., 2000). The correspondence of relative sea level changes with tectonic setting (Figs. 1 and 8), and the increased occurrence of non-storm washover events and earthquake activity suggest that subsidence continues in the San Juan delta. The patterns and differences in relative sea level change indicate that changes are due primarily to recent tectonic activity rather than delta loading and compactation (Restrepo et al., 2002). The above discussion suggests that the San Juan delta has moved from a condition of active growth prior to 1992 to a destructive phase. The hazard is compounded by the incidence of non-storm raised sea levels due to the ENSO events (Fig. 4b). Although the coastline of Mira delta experienced subsidence due to the earthquake in 1979 (Herd et al., 1992; Meyer et al., 1992), the overall decrease in relative sea level may be one of the factors contributing to the protruding behavior during the last five decades.

Along the Caribbean coast, time series of sea level at Cartagena indicate a relative sea level rise of 5.98 mm yr^{-1} (Fig. 8a). Even though the Caribbean deltas have not exhibited erosional trends during the last two decades due to physical processes, many coastal areas between the Atrato and Sinú deltas are experiencing dramatic rates of erosion, up to 50 m yr^{-1} (Correa and Morton, 2006). One of the reasons for this generalized coastal retreat may be due to the geological characteristics of the coast, including sedimentation and compressional tectonics that cause the presence of mud diapirism (Vernette, 1985; Vernette et al., 1992). Also, this shoreline is characterized by series of faulted marine terraces that disappear at the Sinú delta and the Morrosquillo Gulf (Fig. 1f) but reappear to the east of the zone. Based on radiocarbon dates there is a tectonic tilting of 4 mm yr^{-1} where the terraces exist (Page, 1983; Serrano, 2004).

5. Further comparisons and conclusions

Our data indicate that the Mira, Patía, and Magdalena deltas have river power indices ($Q_{max}D_{grd}$) of the same magnitude as the fluvial power of the Paraná, 1.09, and Orinoco, 1.18, and exhibit almost half of the river power of the Amazon, 2.65 (Syvitski, 2005). In addition, Pacific deltas show the highest marine power ($W_a^2 + T_i^2$) of all Colombian deltas, including the larger Magdalena, with values of 9.13, 9.06, and 11.6 in the Mira, Patía, and San Juan deltas, respectively. This was unexpected, as we had anticipated the Magdalena River delta to have the highest marine power of any Colombian delta (Table 4).

Wave climate analysis indicates that the Magdalena delta appear to have the highest nearshore wave-power index of the large deltas along the Atlantic coast of South America (Table 3). It is almost three times greater than the wave-power of the Sao Francisco, 9.97×10^6 erg s^{-1}, and much greater than the wave-power of the Amazon, 1.95×10^6 erg s^{-1}. Compared to deltas worldwide it is of the same magnitude as the nearshore power of the Senegal delta, 37.7×10^6 erg s^{-1}, and greater than those power values observed in major deltas such as the Mississippi, 1.34×10^4 erg s^{-1}, Danube, 1.40×10^4 erg s^{-1}, Ebro, 5.09×10^4 erg s^{-1}, Niger, 6.59×10^5 erg s^{-1}, and Nile, 3.21×10^6 erg s^{-1} (Coleman, 1981).

Although the Pacific and Caribbean coasts of Colombia exhibit extreme geological and oceanographic conditions, including (1) high tectonic activity in the receiving basins, (2) drainage basin divides close to the ocean, (3) narrow continental shelves, (4) moderate to high marine energy conditions, (5) increasing trends in relative sea level, and (6) strong oceanographic manifestations associated with the ENSO cycle, causing sea level rises during El Niño years, the major Colombian rivers have succeeded in building extensive deltas. The Pacific and Caribbean drainage basins are characterized by strong tectonic activity, high rates of precipitation and steep slopes that promote the highest sediment yields of any catchment draining into the Atlantic and Pacific margins, with values ranging from 560 t km^{-2} yr^{-1} in the Magdalena River to 1150 t km^{-2} yr^{-1} in the San Juan River.

The Magdalena is by far the Colombian delta most influenced by wave energy with deep and nearshore wave power values of 45×10^6 erg s^{-1} and 35×10^6 erg s^{-1}, respectively. It also has the lowest wave attenuation ratio of any Colombian delta (Table 3). The steep offshore profile does not attenuate the incoming deep-water waves and results in extremely high wave energy along the shoreline. In contrast, higher attenuation ratios in the Sinú and Atrato deltas correspond with the low offshore profiles. Consequently, the shorelines of these deltas are characterized by marshy indented coastlines.

The river discharge/wave-power climate analysis for the Colombian deltas shows that in the Pacific deltas, wave power and discharge power are out of phase. Probably, this is one of the factors controlling the presence of periodic coastline features such as beach ridge systems. Overall and contrary to what has been documented before (e.g., Martínez et al., 1995, 2000; Vernette et al., 2002), the Pacific deltas exhibit the highest marine energy conditions of all Colombian deltas due to the interplay of moderate wave conditions, meso-tidal ranges, steep subaqueous profiles, and low attenuation indices of deep-water waves.

According to the classification schemes followed in this study (Hori and Saito, 2008; Davies and Hayes, 1984), wave-influenced Colombian deltas are the Magdalena and Sinú, and tide-influenced deltas are the San Juan, Mira, and Patía. Even though there is no Colombian delta being classified as mixed wave and tide-influenced deltas (Fig. 5), the Pacific deltas exhibit definite characteristics of mixed wave and tide-influenced systems due to the presence of barriers and beach ridges (wave energy is high or moderate) and funnel channels with widened mouths kept open by tidal currents (high tidal energy).

Five relationships are proposed between environmental factors and several morphodynamic variables, including

delta area, gradient of the delta plain, and number and width of distributary channels (Tables 1, 4, and 5). Delta area for major Colombian deltas is best predicted by water discharge, while the number of distributary channels is explained by the marine power index and the gradient of the delta plain. The average and total width of distributary channels are largely controlled by the tidal range, indicating the effect of tidal currents in maintaining the channel mouths enlarged. No statistical relationship was found between the number and width of distributary channels and maximum monthly wave height (W_a), water discharge (Q), sediment load (Q_s), river length (L), and the gradient of a delta (D_{grd}).

Currently, the erosional conditions of the San Juan and Magdalena deltas are due to different causes. In San Juan, erosion rates during the last decade have increased due to recent coastal subsidence evidenced by increasing trends in relative sea level and increased erosion of the delta shoreline (with erosion rates as high as $55\ m\ yr^{-1}$). In the Magdalena delta, coastal retreat during the last seven decades has been accentuated by the construction of engineering structures such as jetties that have confined the sediment load in an offshore submarine canyon. In general, the Mira, Atrato, Sinú, and Canal del Dique river deltas exhibit shoreline accretion. The highest progradation rates are observed in the artificial delta of the Canal del Dique, with rates of $100\ m\ yr^{-1}$ during the 1986–2000 yr-period.

Acknowledgements

This study was supported by Instituto Nacional para el Desarrollo de la Ciencia y la Tecnología "Francisco José de Caldas", COLCIENCIAS, grant 1216-05-17616 (Morphodynamics of the Mira River delta, Pacific coast of Colombia), and the Colombian Navy through its research institute CCCP (Centro de Control de Contaminación del Pacífico) in Tumaco, Colombia. Special thanks to Y. Saito, John D. Milliman and Gerardo Perillo for their constructive and valuable comments on this paper.

References

Alvarado, M., 2005. Cartagena y el plan de restauración ambiental del Canal del Dique, y Barranquiilla y las obras de profundización del canal navegable de acceso a la zona portuaria: Visión general. In: Restrepo, J.D. (Ed.), Los Sedimentos del Río Magdalena: Reflejo de la Crisis Ambiental. EAFIT Univ. Press, Medellín, Colombia, pp. 217–254.

Andrade, C.A., 1993. Análisis de la velocidad del viento sobre el Mar Caribe. Boletín Científico CIOH 13, 33–44.

Andrade, C.A., Barton, E.D., 2000. Eddy development and motion in the Caribbean Sea. Journal of Geophysical Research 105, 26191–26201.

Aubrey, D.G., Emery, K.O., Uchupi, E., 1988. Changing coastal levels of South America and the Caribbean region from tide-gauge records. Tectonophysics 154, 269–284.

Bhattacharya, J.P., Giosan, L., 2003. Wave-influenced deltas: geomorphological implications for facies reconstruction. Sedimentology 50, 187–210.

Bretschneider, C.L., 1954. Field investigation of wave energy loss in shallow water ocean waves. US Army Corps Engineers Beach Erosion Board Tech. Special Publication 46, 1–21.

Bretschneider, C.L., Reid, O., 1954. Modification of wave height due to bottom friction, percolation and refraction. US Army Corps Engineers Beach Erosion Board Tech. Special Publication 45, 36 p.

Cane, M.A., 1983. Oceanographic events during El Niño. Science 222, 1189–1210.

Case, J.E., Durán, L.E., López, A., Moore, W.R., 1971. Tectonic investigations in western Colombia and eastern Panamá. Geological Society of America Bulletin 82, 2685–2712.

Cattaneo, A., Correggiari, A., Langone, L., Trincardi, F., 2003. The late-Holocene Gargano subaqueous delta, Adriatic shelf: sediment pathways and supply fluctuations. Marine Geology 193, 61–91.

Coleman, J.M., 1981. Deltas: Processes of Deposition and Models for Exploration, second ed. Burgess Publishing Company, Minneapolis, 102 pp.

Correa, I.D., 1996. Le littoral Pacifique Colombien: interdependance des agents morphostructuraux et hydrodynamiques - Tome 1: texte. Ph.D. dissertation, Universite Bordeaux I, Bordeaux, France, Unpublished, 178 pp.

Correa, I.D., González, J.L., 2000. Coastal erosion and village relocation: a Colombian case study. Ocean and Coastal Management 43, 51–64.

Correa, I.D., Morton, R.A., 2006. Coasts of Colombia. U.S. Department of the Interior USGS. St. Petersburg, Florida. Available from: <http://coastal.er.usgs.gov/coasts-colombia/index.html>.

Davies, R.A., Hayes, M.O., 1984. What is a wave dominated coast? Marine Geology 60, 313–329.

Day, J.W., Pont, D., Hensel, P.F., Ibañez, C., 1995. Impacts of sea-level rise on deltas in the Gulf of Mexico and the Mediterranean: the importance of pulsing events to sustainability. Estuaries 18, 636–647.

Defant, A., 1960Physical Oceanography, vol. 2. Pergamon Press, Oxford, 598 pp.

Emery, K.O., Aubrey, D.G., 1991. Sea Levels, Land Levels, and Tide Gauges. Springer, New York, 226 pp.

Enfield, D.B., Allen, J.S., 1980. On the structure and dynamics of monthly mean sea levels anomalies along the Pacific coast of North and South America. Journal of Physical Oceanography 10, 557–578.

Ericson, J.P., Vörösmarty, C.J., Dingman, S.L., Ward, L.G., Meybeck, M., 2006. Effective sea-level rise and deltas: causes of change and human dimension implications. Global and Planetary Change 50, 63–82.

Franco, A.S., 1988. Tides: Fundamentals, analysis and predictionFundacao Centro-Tecnologico de Hidraulica (FCTH). São Paulo, Brazil, 249 pp.

Franco, A.S., 1992. Tides Programs for Prediction and Analysis: Manual. São Pablo, Brazil, 45 pp.

Galloway, W.E., 1975. Processes framework for describing the morphologic and stratigraphic evolution of deltaic depositional systems. In: Broussard, M.L. (Ed.), Deltas: Models for Exploration. Houston Geological Society, Houston, pp. 87–98.

González, J.L., Correa, I.D., 2001. Late Holocene evidence of coseismic subsidence on the San Juan delta, Pacific coast of Colombia. Journal of Coastal Research 17, 459–467.

Gould, H.R., 1979. The Mississippi delta complex. SEPM Special Publication 15, pp. 3–30.

Glantz, M.H., 1997. Currents of Change, El Niño's Impact on Climate and Society. Cambridge University Press, Cambridge, 194 pp.

Harris, P.T., Hughes, M.G., Baker, E.K., Dalrymple, R.W., Keene, J.B., 2004. Sediment transport in distributary channels and its export to the pro-deltaic environment in a tidally dominated delta: Fly River, Papua New Guinea. Continental Shelf Research 24, 2431–2454.

Herd, D.G., Youd, T.L., Meyer, H., Arango, J.L., Person, W.J., Mendoza, C., 1992. The great Tumaco, Colombia earthquake of December 1979. Science 211, 441–445.

Hori, K., Saito, Y., Shao, Q., Wang, P., 2002. Architecture and evolution of the tide-dominated Changjiang (Yangtze) river delta, China. Sedimentary Geology 146, 249–264.

Hori, K., Saito, Y., 2008. Classification, architecture and evolution of large river deltas. In: Gupta, A. (Ed.), Large Rivers: Geomorphology and Management. John Wiley and Sons, pp. 214–231.

Hovius, N., Stark, C.P., Allen, P.A., 1997. Sediment flux from a mountain belt derived by landslide mapping. Geology 25, 231–234.

Hovius, N., Stark, C.P., Tutton, M.A., Abbott, L.D., 1998. Landslide-driven drainage network evolution in a pre-steady-state mountain belt: Finisterre Mountains, Papua New Guinea. Geology 26, 1071–1074.

IDEAM, 1995. Estadísticas Hidrológicas de Colombia (1990–1993). Tomos I–II. Bogotá, Diego Samper Ediciones, 1097 pp.

INGEOMINAS, 2005. Sismicidad registrada por la Red Sismológica Nacional de Colombia (Junio de 1993 a Diciembre de 2003). Mapa a escala 1:2.000.000.

Kanes, W.H., 1970. Facies and development of the Colorado River delta in Texas. SEPM Special Publication 15, pp. 78–106.

Kjerfve, B., 1981. Tides of the Caribbean Sea. Journal of Geophysical Research 86, 4243–4247.

Kjerfve, B., Wiebe, W.J., Kremer, H.H., Salomons, W., Marshall Crossland J.-I. (Eds.), 2002. Caribbean basins: LOICZ global change assessment and synthesis of river catchment/island–coastal sea interaction and human dimensions. LOICZ Reports and Studies, No. 27, Texel, The Netherlands.

Kellogg, J.N., Mohriak, W.U., 2001. The tectonic and geological environment of coastal South America. In: Seeliger, U., Kjerfve, B. (Eds.), Coastal Marine Ecosystems of Latin America. Springer Verlag, Berlin, Heilderberg, pp. 2–16.

Kellogg, J.N., Vega, V., 1995. Tectonic development of Panama, Costa Rica, and the Colombian Andes: Constrains from Global Positioning System geodetic studies and gravity, Geologic and Tectonic Development of the Caribbean plate boundary in southern Central America. In: Mann, P. (Ed.), GSA Special Paper 295, pp. 75–90.

Kolla, V., Buffler, T., 1984. Seismic stratigraphy and sedimentation of Magdalena Fan, Southern Colombia basin, Caribbean Sea. A.A.P.G. Bulletin 68, 316–332.

Kuehl, S.A., Levy, B.M., Moore, W.S., Allison, M.A., 1997. Subaqueous of the Ganges–Brahmaputra river system. Marine Geology 144, 81–96.

Latrubesse, E.M., Stevaux, J.C., Sinha, R., 2005. Tropical rivers. Geomorphology 70, 187–206.

Lockridge, P.A., Smith, R.H., 1984. Tsunamis in the Pacific Basin 1900–1983: Map (1:17,000.000). National Geophysical Data Center, Boulder, Colorado.

Martínez, J.O., González, J.L., Pilkey, O.H., Neal, W.J., 1995. Tropical barrier islands of Colombia's Pacific coast. Journal of Coastal Research 11, 432–453.

Martínez, J.O., González, J.L., Pilkey, O.H., Neal, W.J., 2000. Barrier island evolution on the subsiding central Pacific coast, Colombia, S.A. Journal of Coastal Research 16, 663–674.

Meade, R.H., 1988. Movement and storage of sediment in river systems. In: Lerman, A., Maybeck, M., (Eds.), Physical and Chemical Weathering in Geochemical Cycles. NATO ASI Series C in Mathematical and Physical Sciences 51, pp. 165–179.

Meyer, H., Mejía, J.A., Velásquez, A., 1992. Informe preliminar sobre el terremoto del 19 de noviembre de 1991 en el Departamento del Chocó. Publicaciones Ocasionales OSSO, Universidad del Valle, Cali, Colombia, 13 pp.

Milliman, J.D., Syvitski, P.M., 1992. Geomorphic/tectonic control of sediment transport to the ocean: the importance of small mountainous rivers. The Journal of Geology 100, 525–544.

Morton, R.A., González, J.L., López, G.I., Correa, I.D., 2000. Frequent non-storm washover of barrier islands, Pacific coast of Colombia. Journal of Coastal Research 16, 82–87.

National Oceanic and Atmospheric Administration-NOAA, 2005. Monthly atmospheric and SST indices. National Oceanic and Atmospheric Administration, National Weather Service-Climate Prediction Center. Available from: <http://www.cpc.noaa.gov/data/indices>.

Neal, W.J., González, J.L., 1990. Coastal photograph. Journal of Coastal Research 6, 800.

Nittrouer, C.A., Kuehl, S.A., Figueiredo, A.G., Allison, M.A., Sommerfield, C.K., Rine, J.M., Faria, E.C., Silveira, O.M., 1996. The geological record preserved by Amazon shelf sedimentation. Continental Shelf Research 16, 817–841.

Orton, G.J., Reading, H.G., 1993. Variability of deltaic processes in terms of sediment supply, with particular emphasis on grain size. Sedimentology 40, 475–512.

Page, W.D., 1983. Holocene deformation of the Caribbean coast, northwestern Colombia. Woodward and Clyde Consultants, San Francisco, 25 pp.

Pennington, W.D., 1981. Subduction on the eastern Panama Basin and seismotectonics of Northwestern South America. Journal of Geophysical Research 86, 10753–10770.

Postma, G., 1995. Sea-level-related architectural trends in coarse-grained delta complexes. Sedimentary Geology 98, 3–12.

Pugh, D.T., 1987. Tides, surges and sea-level: a handbook for engineers and scientists. Wiley, New York, 472 pp.

Pugh, D.T., 2004. Changing Sea Levels. Effects of Tides, Weather and Climate. Cambridge University Press, Cambridge, UK, 265 pp.

Quinn, W.H., Zopf, D.O., Short, K.S., Kuo Yang, R.T.W., 1978. Historical trends and statistics of the Southern Oscillation, El Niño, and Indonesian droughts. Fishery Bulletin 76, 663–678.

Restrepo, J.D., Kjerfve, B., 2000a. Water discharge and sediment load from the western slopes of the Colombian Andes with focus on Rio San Juan. The Journal of Geology 108, 17–33.

Restrepo, J.D., Kjerfve, B., 2000b. Magdalena River: interannual variability (1975–1995) and revised water discharge and sediment load estimates. Journal of Hydrology 235, 137–149.

Restrepo, J.D., Kjerfve, B., 2002. San Juan River delta, Colombia: tides, circulation, and salt dispersion. Continental Shelf Research 22, 1249–1267.

Restrepo, J.D., Kjerfve, B., Correa, I.D., González, J.L., 2002. Morphodynamics of a high discharge tropical delta, San Juan River, Pacific coast of Colombia. Marine Geology 192, 355–381.

Restrepo, J.D. (Ed.), 2005. Los sedimentos del Río Magdalena: reflejo de la crisis ambiental. Eafit University Press, Medellín, Colombia, p. 267.

Restrepo, J.D., Syvitski, J.P.M., 2006. Assessing the effect of natural controls and land use change on sediment yield in a major Andean river: the Magdalena drainage basin, Colombia. Ambio 35, 44–53.

Restrepo, J.D., Zapata, P., Díaz, J.M., Garzón, J., García, C., 2006. Fluvial fluxes into the Caribbean Sea and their impact on coastal ecosystems: the Magdalena River, Colombia. Global and Planetary Change 50, 33–49.

Restrepo, J.D., 2007. Applicability of LOICZ catchment-coast continuum in a major Caribbean basin: the Magdalena River, Colombia. Estuarine, Coastal and Shelf Science. doi:10.1016/j.ecss.2007.09.014.

Shepard, F.P., 1973. Sea floor off the Magdalena delta and Santa Marta area, Colombia. Geological Society of America Bulletin 84, 1955–1972.

Shepard, F.P., Dill, R.F., Heezen, B.C., 1968. Diapiric intrusions in foreset slope sediments off Magdalena delta, Colombia. American Association of Petroleum Geologists Bulletin 52, 2197–2207.

Schurman, P., 1941. Manual of harmonic analysis and prediction of tides. Coast and Geodetic Survey Special Publication, vol. 98. United States Printing Office, Washington, DC., 313 pp.

Schwing, F.B., Kjerfve, B., Sneed, J., 1983. Nearshore coastal currents on the South Carolina continental shelf. Journal of Geophysical Research 88, 4719–4729.

Serrano, B.E., 2004. The Sinú river delta on the northwestern Caribbean coast of Colombia: bay infilling associated with delta development. Journal of South American Earth Sciences 16, 639–647.

Snow, J.W., 1976. The climate of northern South America: Colombia. In: Schwerdtfeger, W. (Ed.), Climates of South and Central America. Elsevier Scientific Publishing Company, Amsterdam, pp. 358–379.

Soeters, R., Gómez, J., 1985. Contribución del estudio geomorfológico para el proyecto de canales y esteros. In: Rizo, D., Contreras, R. (Eds.), Estudio del Impacto Ambiental para la Proyección y Canalización de Esteros. Cali, CVC-PLAIDECOP, pp. 285–337.

Stallard, R.F. 1988. Weathering and erosion in the humid tropics. In: Lerman, A., Meybeck, M. (Eds.), Physical and Chemical Weathering in Geochemical Cycles. NATO ASI Series C in Mathematical and Physical Sciences 51, pp. 225–246.

Storms, J.E.A., Hoogendoorn, R.M., Dam, R.A.C., Hoitink, A.J.F., Kroonenberg, S.B., 2005. Late-Holocene evolution of the Mahakan delta East Kalimantan, Indonesia. Sedimentary Geology 180, 149–166.

Syvitski, J.P.M., 2005. The Morphodynamics of Deltas and their Distributary Channels. Online, http://www.criba.edu.ar/scorwg122/reports/RCEMpaper.pdf.

Syvitski, J.P.M., Kettner, A.J., Correggiari, A., Nelson, B.W., 2005a. Distributary channels and their impact on sediment dispersal. Marine Geology 222–223, 75–94.

Syvitski, J.P.M., Vörösmary, C.J., Kettner, A., Green, P., 2005b. Impacts of humans on the flux of terrestrial sediment to the global coastal ocean. Science 308, 376–380.

Syvitski, J.P.M., Milliman, J.D., 2007. Geology, geography and humans battle for dominance over the delivery of fluvial sediment to the Coastal Ocean. The Journal of Geology 115, 1–19.

Tabares, N., Soltau, J.M., Díaz, J., 1996. Caracterización geomorfológica del sector suroccidental del Mar Caribe. Boletín Científico CIOH 17, 3–16.

USACE, 2002. Coastal engineering manual. Department of the Army, U.S. Army Corps. of Engineers, Washington, DC, CD-ROM, 153 MB.

Velásquez, A., Meyer, H., Marin, W., Ramírez, F., Drews, A.D., Campos, A., Hermelin, M., Bender, S., Arango, M., Serje, J., 1994. Planificación regional del occidente colombiano bajo consideración de las restricciones por amenazas. Memorias del Taller OEA sobre planificación del desarrollo regional y prevención de desastres. Publicación Especial, 1–36.

Vernette, G. 1985. La plate-forme continentale caraibe de Colombie (du débouché du Magdalena au Golfe de Morrosquillo). Importance du diapirisme argileux sur la morphologie et la sedimentation. Ph.D. dissertation, Universite Bordeaux I, Bordeaux, Unpublished, 387 pp.

Vernette, G., Gayet, J., Echeverry, C.M., Piedrahita, I., Correa, I.D., 2002. Introducción a los ambientes deltaicos: morfología y sedimentación. In: Correa, I.D., Restrepo, J.D. (Eds.), Geología y Oceanografía del Delta del Río San Juan: Litoral Pacífico Colombiano. Fondo Editorial Universidad EAFIT, Medellín, pp. 22–53.

Vernette, G., Mauffret, A., Bobier, C., Briceno, L., Gayet, J., 1992. Mud diapirism, fan sedimentation and strike-slip faulting, Caribbean Colombian margin. Tectonophysics 202, 335–349.

West, R.C., 1957. The Pacific Lowlands of Colombia – A Negroid Area of the American Tropics. Baton Rouge, Louisiana University Press, 278 pp.

Wiegel, R.L., 1948. Oscillatory waves. U.S. Army, Beach Erosion Board Bulletin, Special Issue 1.

Woodruff, S.D., Slutz, J.R., Jenne, R.L., Steurer, P.M., 1987. A Comprehensive Ocean-Atmosphere Data Set Release 1 (1854–1979). Bulletin American Meteorological Society 68, 1239–1250.

Woodruff, S.D., Lubker, S.J., Wolter, K., Worley, S.J., Elms, J.D., 1993. Comprehensive Ocean-Atmosphere Data Set (COADS) Release 1a: 1980–1992. Earth System Monitor 4, 1–8.

Woodruff, S.D., Diaz, H.F., Elms, J.D., Worley, S.J., 1998. ICOADS Release 2 data and metadata enhancements for improvements of marine surface flux fields. Physics and Chemistry of the Earth 23, 517–527.

Wright, L.D., 1977. Sediment transport and deposition at river mouths: a synthesis. Geological Society of America Bulletin 88, 857–868.

Wright, L.D., Coleman, J.M., 1971. Effluent expansion and interfacial mixing in the presence of a salt wedge, Mississippi River delta. Journal of Geophysical Research 76, 8649–8661.

Wright, L.D., Coleman, J.M., 1972. River delta morphology: wave climate and role of the subaqueous profile. Science 176, 282–284.

Wright, L.D., Coleman, J.M., 1973. Variations in morphology of major river deltas as functions of ocean wave and river discharge regimes. Bulletin of the American Association of Petrologists and Geologists 57, 370–398.

Wright, L.D., Coleman, J.M., 1974. Mississippi River mouth processes: effluent dynamics and morphologic development. The Journal of Geology 82, 751–778.

Wyrtki, K., 1975. El Niño – The dynamic response of the equatorial Pacific Ocean to atmospheric forcing. Journal of Physical Oceanography 5, 572–584.

Wyrtki, K., 1977. Sea level during the 1972 El Niño. Journal of Physical Oceanography 7, 779–787.